POTENTIAL OF A BIOSCAFFOLD TO ENHANCE THE HEALING OF THE MCL FOLLOWING A MOP-END TEAR: AN ANIMAL MODEL STUDY

by

Noah Peter Papas

B.S. in Engineering Science and Mechanics, Virginia Polytechnic Institute and State University,

2005

Submitted to the Graduate Faculty of

The School of Engineering in partial fulfillment

of the requirements for the degree of

Master of Science in Bioengineering

University of Pittsburgh

2007

UNIVERSITY OF PITTSBURGH

SCHOOL OF ENGINEERING

This thesis was presented

by

Noah P. Papas

It was defended on

May 3, 2007

and approved by

Steven D. Abramowitch, Ph.D., Research Assistant Professor, Department of Bioengineering

Steven Badylak, D.V.M., M.D., Ph.D., Research Professor, Department of Surgery
Director of Tissue Engineering, McGowan Institute for Regenerative Medicine

Thesis Advisor: Savio L-Y. Woo, Ph.D., D.Sc. (hon.), University Professor of Bioengineering, Departments of Bioengineering, Mechanical Engineering, and Rehabilitation Science & Technology

POTENTIAL OF A BIOSCAFFOLD TO ENHANCE THE HEALING OF THE MCL FOLLOWING A MOP-END TEAR: AN ANIMAL MODEL STUDY

Noah P. Papas, M.S.

University of Pittsburgh, 2007

Isolated medial collateral ligament (MCL) injuries occur frequently (95,000 per year in the US) and heal with conservative treatment. Long-term clinical outcome is generally excellent because the structural properties of the Femur-MCL-Tibia complex (FMTC) naturally return to normal especially the stiffness. However, the quality of the healing ligament, as described by its histomorphological appearance, as well as biochemical, mechanical, and viscoelastic properties, remain poor [37, 70, 108, 109, 116]. Functional tissue engineering techniques such as the use of extracellular matrix (ECM) bioscaffolds have shown promise in improving healing of soft tissues after injury. In particular, small intestine submucosa (SIS) is especially attractive due to its chemoattractant properties, organized fiber alignment, and natural concentration of growth factors [9, 13, 48]. The objective of this thesis is to use SIS to improve MCL healing in a clinically relevant injury model.

Sixteen New Zealand white rabbits were subjected to a mop-end tear (Weiss et al. 1991) in order to simulate a clinically relevant injury, which included damage to the ligament insertion sites, over-stretching of collagen fibers, and a frayed appearance of the torn ligament ends. After 12 weeks of healing, seven rabbits per group were euthanized and subjected to a well-established biomechanical testing protocol [111], including a load to failure test. The remaining rabbits (n=2 per group) were evaluated histologically.

It was found that SIS treatment resulted in a marked improvement for the tangent modulus of the healing MCL midsubstance over non-treatment (404 ±120 MPa vs. 273 ± 91 MPa, respectively, $p<0.05$). However, this difference did not translate into a change in the measured structural properties of the FMTC. Nearly half of the specimens in each treatment group failed at the tibial insertion, this indicates asynchronous healing between the ligament insertion and midsubstance.

In conclusion, these results confirm SIS enhances the quality of the healing MCL. SIS positively effects the local healing response of an MCL regardless of injury model. This work provides a basis to explore the effect of applying SIS to ligaments which do not heal well naturally, such as the anterior cruciate ligament.

TABLE OF CONTENTS

LIST OF TABLES

LIST OF FIGURES

PREFACE

On April 16th, 2007 I turned in this thesis to my committee. Also on that day, a troubled young man killed 33 people including himself and two professors who I was acquaintances with on the campus of Virginia Tech, my undergraduate institution. Not only did this occur on a campus where I spent 4 years, but in the building where I spent a majority of my junior and senior years, Norris Hall. Norris Hall is the home of Engineering Science and Mechanics Department, and by extension a home to me. The events of that day shocked and saddened me to a great degree, and I am merely an alumni of the department and school. I cannot fathom how it effected those students and professors in the classrooms, in the building or on campus that day, let alone the families and close friends of the victims. I think though that can be the enduring message of the massacre, not the senseless killing, but rather the amazing way the entire Hokie nation embraced each other as a community, to support the memory of the victims, and there grieving families. We all cried, we all cheered, we all hugged, emailed and called each other, and we all donated, together. The university's motto *UT PROSIM*, Latin for that I may serve rang true as Virginia Tech showed the world what it means to serve each other, what it means to be a community. WE ARE VIRGINIA TECH!

At this time it is fitting that I acknowledge all those who have taught, guided and helped me through these difficult two years. Each one has had a part in helping me become the scientist, engineer and professional I am today. First, I would like to thank my advisor Dr. Woo

for giving me this amazing opportunity to work under his tutelage. I feel as if he took a chance with me, taking me on and funding me as just a Master's student. I hope that I have fulfilled his expectations, and fully taken advantage of this opportunity. I also would like to thank Steve (Dr. Abramowitch), for always having an open door, to discuss, tensile tests, or emotional hardships. This thesis, and quite honestly graduate school, would have been impossible with out his guidance. I would also like to acknowledge the third member of my committee Dr. Steven Badylak, I am awed and honored to have him as the foremost expert on SIS critique my efforts which use SIS as the MCL injury treatment of choice.

I need to also thank the clinicians who made this study possible, by doing the surgeries, sacrifices and dissections; Drs. Sinan Karaglou, Ping-Chen Lui and Chin-Yi Chou. Especially, Sinan for being the older brother I never had (even though he is closer to the age of my father).

In addition, all those who I have worked with at the MSRC, namely members of the Tissue Mechanics and Mechanobiology groups, my mentor Dan Moon, close friends Alex, Sabrina, Matt, and Laurie, all of the new first years, my undergrads, and my summer student Tobias.

I would also like to thank my family for their love and support, especially my mom and dad and my sisters, and my Papou' who is my hero, and engineering example.

Finally, I would like to thank God, for the talents and abilities He has given me and allowed me to complete this work. Hopefully, this work will in some way serve others, and in doing so glorify Him.

LIST OF NOMENCLATURE

ACL	-	Anterior cruciate ligament
CSA	-	Cross sectional area
ECM	-	Extracellular Matrix
FMTC	-	Femur-MCL-Tibia complex
FTE	-	Functional tissue engineering
GAGs	-	Glycosaminoglycans
H&E	-	Hematoxylin and eosin
IACUC	-	Institutional Animal Care and Use Committee
SIS	-	Small intestine submucosa
LCL	-	Lateral collateral ligament
MCL	-	Medial collateral ligament
NT	-	Non-treated
PCL	-	Posterior cruciate ligament
QLV	-	Quasi-linear viscoelasticity
TEM	-	Transmission electron microscopy
V-V	-	Varus-valgus

1.0 MOTIVATION

In the United States there are nearly 100,000 cases of isolated medial collateral ligament (MCL) tears plus nearly 50,000 combined MCL+ACL (anterior cruciate ligament) injuries annually [76]. Isolated MCL tears heal with conservative treatment and the structural properties of the bone-ligament-bone complex can return to near normal values in the long-term. However, the quality of the healing tissue, described by the viscoelastic and mechanical properties, as well as the ultra-structure and biochemical composition of the healing MCL, remains inferior for years [45, 108, 118]. In other words, the quality of the healing tissue decreases, and the ligament responds through hypertrophy of that inferior tissue in order to restore function.

In the case of a combined MCL+ACL injury, the clinical management has been debated [5, 28, 29, 98, 120-122]. The current consensus is to treat the MCL conservatively and reconstruct the ACL [29]. However, because the function of both ligaments directly affects the other [55], questions remain as to the timing of the surgical repair and rehabilitation following this type of injury [5, 28, 29, 98, 120-122]. It is also known that even after ACL reconstruction the healing MCL tissue in a combined injury is not comparable to that of an isolated MCL injury [90].

Functional tissue engineering (FTE) techniques have shown promise to improve the properties of healing ligaments and tendons. The use of decellularized porcine small-intestinal submucosa (SIS) as a bioscaffold is especially attractive. SIS offers many positive advantages,

including resistance to bacterial infection, promotion of angiogenesis, preferred alignment, and the presence of growth factors [14, 62, 105]. Previous animal studies have shown that the *in vivo* application of SIS improves healing of the Achilles tendon [14] and rotator cuff [25]. In our research center, we have used SIS to enhance MCL healing in a gap injury rabbit model. This treatment improved mechanical properties of the healing MCL at 12 and 26 weeks when compared to non-treatment. Other important results were a reduction of the collagen V/I ratio which leads to an increase in collagen fibril diameter and an improved fiber organization [67, 79]. Both of these were displayed histologically and led to the improvement of the tissue's mechanical properties. It was hypothesized that the unique biological properties of the SIS, such as growth factors and highly aligned ECM, decreased collagen V/I ratio. A reduction in collagen V increases collagen fibril diameter [83]. At the same time, the SIS guides the cells to produce a more aligned matrix through contact guidance [107]. These experiments were designed using a severe "gap injury" model in which 6 mm of MCL tissue was excised. This was done to better elucidate the positive effects of SIS. However, with this injury model no damage was done to the insertion sites, there was no overstretching of the collagen fibers, nor were there frayed edges of the torn ligament ends.

The main objective of this thesis is to examine the improvement to the outcome of ligament healing after a clinically relevant injury model and treatment with SIS. **With the knowledge of ligament healing acquired in this thesis there is a potential to extend the use of SIS in other ligaments or tendons such as the ACL or patellar tendon where the healing response is less than favorable. Thus, the work is significant to both basic science and the clinical realm.**

2.0 BACKGROUND

2.1 ANATOMY AND STRUCTURE OF MCL

The MCL is one of 4 major ligaments which stabilize the tibiofemoral knee joint. It along with the lateral collateral ligament (LCL), are considered extra-articular as they are outside of the joint capsule. These ligaments as well as the intra-articular passive stabilizers the (ACL and posterior cruciate ligament [PCL]) are shown in Figure 1. The MCL connects the femur to the tibia on the medial side of the knee. As such its main purpose is to stabilize valgus rotation of the tibia and femur.

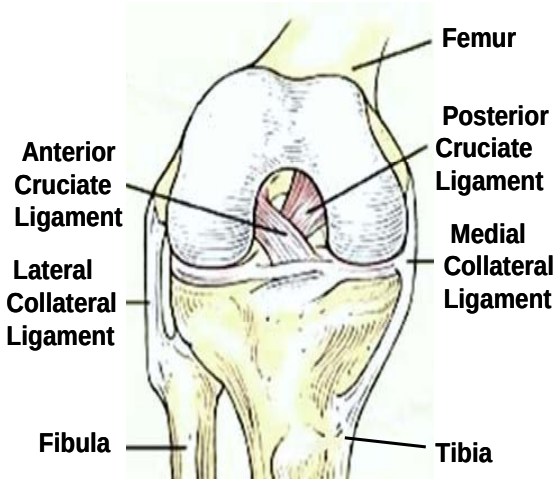

Figure 1. The anterior cruciate ligament (ACL), posterior cruciate ligament (PCL), medial collateral ligament (MCL), and lateral collateral ligament (LCL) of the right knee.

The MCL is predominantly made of a highly organized extracellular matrix (ECM) of densely packed collagen fibers (shown in pink in Figure 2) and interspersed cells named fibroblasts (the nuclei of which are stained blue in Figure 2). In a healthy MCL, the fibroblasts are spindle-shaped and aligned along the direction of loading. The collagen fibers are oriented in the direction of normal loading as well. These fibers follow an architectural hierarchy with tropocollagen as the basic molecular component, and systematically arranged into microfibrils, subfibrils, fibrils, and fibers. Inspection of an MCL under a microscope reveals an undulating crimp pattern which straightens easily when a force is applied. Figure 2 shows a histological section of a rabbit medial collateral ligament.

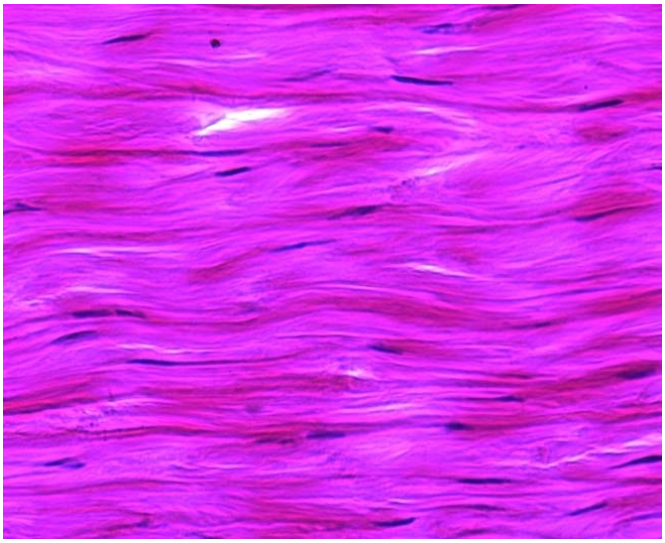

Figure 2. Histological image of rabbit medial collateral ligament showing highly organized collagen fibers and the crimp pattern (Hematoxylin & Eosin staining).

Another important functional area of the MCL are its insertion sites. The insertions of ligaments into bone distribute and dissipate loads from soft to hard tissues. There are two types of insertions--direct and indirect-and the MCL uses both types. The MCL femoral insertion site is a direct insertion which the transition of fibers from ligament to bone occurs in four distinct phases: ligament, fibrocartilage, mineralized fibrocartilage, and bone (Figure 3 A) [24, 33, 116].

The middle two phases, uncalcified and calcified fibrocartilage, minimize stress concentrations [116]. The tibial insertion of the MCL is an indirect insertion. The indirect insertion is more complex than the direct insertion as it contains distinct superficial and deep fibers. The superficial fibers are connected to the periosteum (Figure 3 B) [24, 63, 116], while the deeper fibers, sometimes called the Sharpey fibers, are anchored directly to the bone.

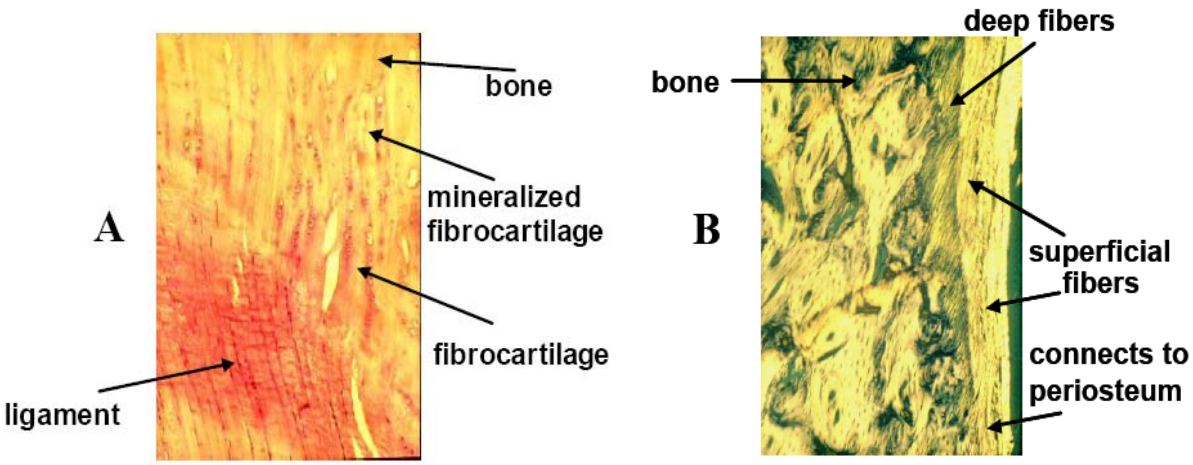

Figure 3. Morphology of the insertion sites in a ligament. (A) Direct insertion; (B) Indirect insertion.

At the molecular level, Type I collagen is the major component of all fibers and is primarily responsible for an MCL's tensile strength [36]. Other collagen types, such as type III, V, VI, IX, X, XI and XII appear in minor amounts; however, they play a significant role in fibrillogenesis and homeostasis. Types III and V collagen have been implicated in the regulation of collagen fibril diameter and organization [15, 16, 69], and they also function in wound healing where their levels were found to be elevated [83]. Research has shown that Type XII collagen provides lubrication between collagen fibrils. Types IX, X, and XI collagen have been identified to coexist with Type II collagen at the fibrocartilaginous zone of the ligament-bone interface [39,

84, 85] and are believed to have the function of minimizing the stress concentrations when loads are transmitted from soft tissue into bone [24, 73, 112].

Elastin, another fibrous protein present in ligaments (usually <1% of the dry weight), allows the tissue to return to its pre-stretched length following physiological loading. Other constituents include glycoprotiens (e.g., fibronectin), proteoglycans, and glycosaminoglycans (GAGs). Although they exist in relatively small amounts, they have a significant function in the formation, organization, and maintenance of the ECM [36]. They also play a role in water retention, which is correlated with viscoelastic behavior [22].

2.2 BIOMECHANICAL PROPERTIES OF LIGAMENTS

Since the major function of ligaments (like the MCL) is to resist tensile loads, it is of clinical importance to characterize their biomechanical behavior and their relative contribution to joint kinematics. Uniaxial tensile tests are the common way to obtain structural and mechanical properties [111]. Generally, when a bone-ligament-bone complex is tested, the resulting load-elongation curve exhibits non-linearity, including an initial non-linear region called the "toe region." During this stage, in which normal joint movements occur, the progressive straightening and stretching of an increasing number of fibers takes place (fiber recruitment). Once a majority of the fibers are recruited with the increasingly applied load, the curve gradually transitions to a "linear" region where the slope becomes constant. This biphasic behavior allows ligaments to maintain normal joint laxity in response to low loads (low stiffness toe region), and to prevent excessive joint displacement in response to high loads (high stiffness linear region).

Finally, a continuous increase in loading will eventually cause the specimen to fail. Figure 4 (A) shows a typical non-linear load-elongation curve for a bone-ligament-bone complex.

The load-elongation curves represent the tensile behavior of the whole structure including their insertions to bone. Structural properties are described by the following parameters:

- Stiffness (N/mm): The relationship between load and elongation defined as the slope of the linear portion of the curve.
- Ultimate Load (N): Maximum value of load before failure.
- Ultimate Elongation (mm): Maximum elongation before failure.
- Energy Absorbed to Failure (N mm): The area under the load-elongation curve which represents energy stored in the complex before failure.

To assess the quality of the ligament substance, mechanical properties as represented by a stress-strain curve must be obtained. These properties reflect collagen fiber organization and orientation, fibril diameter, collagen density, as well as the microstructure among other things. Mechanical properties are determined by normalizing the load to the cross sectional area (stress, σ) and normalizing the change in elongation to the ligament's original length (strain, ε). Cross sectional area can be obtained by a variety of methods, but it is best to use a non-contact method such as a laser micrometer system [110] or laser reflectance system [77]. For strain, video cameras and a video dimension analysis system are used to track the position of contrasting markers placed on the ligament [96]. Thus, measuring stress and strain is possible without making physical contact with the soft tissue. In order to avoid the contribution of the insertion sites, it is important to use the stress-strain relationship of the midsubstance of the ligament or tendon. A typical stress-strain curve for a ligament midsubstance is shown in Figure 4 (B). Mechanical properties of the ligament or tendon are described by the following parameters:

- Tangent Modulus (MPa): The relationship between stress and strain defined by the slope of the linear portion of the stress-strain curve.
- Ultimate Tensile Strength (MPa): Also called ultimate stress, it is the highest stress experienced by the tissue before failure.
- Ultimate Strain (unitless or %): The strain in the ligament at failure.
- Strain Energy Density (MPa): The area under the stress strain curve, and can be described as the amount of energy absorbed per unit volume.

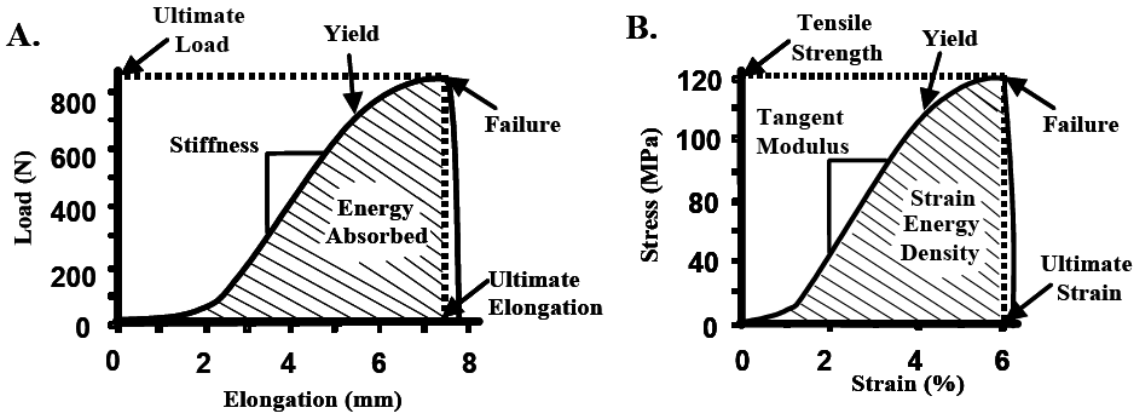

Figure 4. The biomechanical properties of bone-ligament-bone complex. (A) A typical load-elongation curve; (B) A typical stress-strain curve for a ligament midsubstance.

Ligaments also exhibit complex time- and history-dependent viscoelastic properties which reflect complex interactions between proteoglycan molecules, water, collagen, and other structural components of soft tissues. When a ligament is pulled to a particular elongation, either once or repeatedly in cycles, the stress in the tissue decreases with time. Specifically, this means that when soft tissue is elongated to a given length and remains at this same length over time, the load supported by the tissue progressively declines. This behavior is referred to as a stress relaxation (Figure 5 A). Conversely, when a viscoelastic material is subjected to a constant

stress it elongates with time. This behavior is called creep (Figure 5 B). During cyclic loading, an elastic material follows the same stress-strain curve, whereas a viscoelastic material displays a hysteresis loop-a phenomenon in which the load-elongation curve differs during loading and unloading and results in net internal energy loss (Figure 6). Due to these properties, the shape of the load-elongation curve of the bone-ligament-bone complex depends on the previous loading history and the time over which the load is applied. However, over the course of several cycles, the area of hysteresis is reduced and the curves become more repeatable. Because the mechanical behavior of a tissue tested after the first cycle will differ from that of a tissue tested at the tenth cycle, the specimen must be preconditioned by a number of cycles to obtain more consistent data.

The viscoelastic behavior of ligaments has important physiological and clinical implications. During walking or running, ligaments undergo cyclic loading. As a result, cyclic stress relaxation will effectively lower the stress in the ligament substance [113, 117]. This phenomenon may help prevent fatigue failure of ligaments. Repetitive stress causes failure at a much lower load than that required to cause failure from a single application of stress. Similarly, cyclic creep can be used to demonstrate how warm-up exercises and stretching can increase the flexibility of a joint, as a constant applied stress during stretching increases the length of the ligaments.

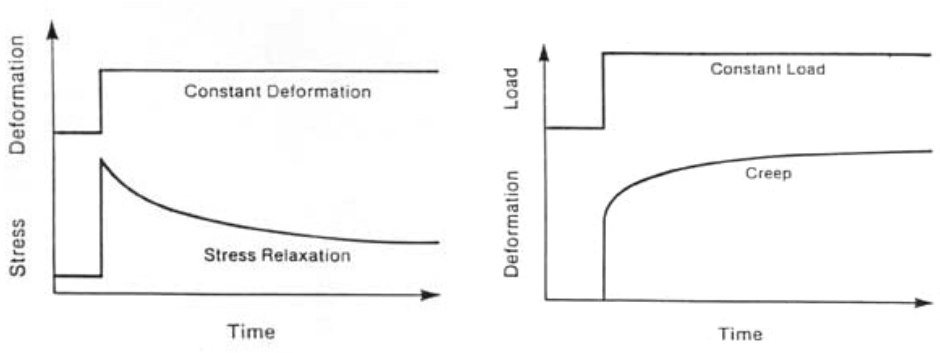

Figure 5. (A) Schematic representation of stress-relaxation; (B) Schematic representation of creep.

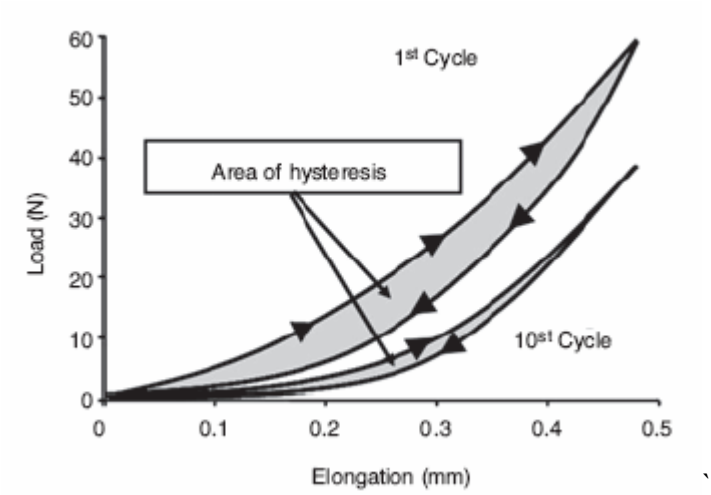

Figure 6. The loading and unloading curves for a ligament do not follow the same path, forming a hysteresis loop. Note the decrease in the area of hysteresis by the tenth cycle of loading and unloading.

In order to model this behavior many theories have been developed from the simple Maxwell model [40], to more complex non-linear models [40, 47, 93, 94]. The quasi-linear viscoelastic (QLV) theory developed by Fung [40, 41] has been successfully applied to describe the time- and history-dependent viscoelastic properties of soft tissues [19, 58, 100, 123], especially ligaments [4, 42, 61, 114] and tendons [30, 104]. The theory assumes a separable non-linear elastic response and a separate time-dependent relaxation function can be combined in a convolution integral to result in a 1-D general viscoelastic model expressed as follows:

$$\sigma(t) = \int_{-\infty}^{t} G(t-\tau)\frac{\partial \sigma^e(\varepsilon)}{\partial \varepsilon}\frac{\partial \varepsilon}{\partial \tau}\partial\tau \quad \textbf{(1)}$$

The elastic response is a strain dependent function and can be written:

$$\sigma^e(\varepsilon) = A(e^{B\varepsilon} - 1) + k. \quad \textbf{(2)}$$

Using Fung's generalized relaxation function based on the assumption of a continuous relaxation spectrum, the time-dependent reduced relaxation function, G(t) [40, 41], takes the form

$$G(t) = \frac{1 + C[E_1(t/\tau_2) - E_1(t/\tau_1)]}{1 + C\ln(\tau_2/\tau_1)} \quad \textbf{(3)}$$

Where $E_1 = \int_y^{\infty} \frac{e^{-z}}{z} dz$, yielding parameters C, τ_1, and τ_2 [41].

Thus, this approach yields five physically significant constants: A, B, C, τ_1, and τ_2. A*B represents the initial slope of the instantaneous elastic response, and B correlates with the non-linearity of the instantaneous elastic response. C is a scaling parameter that is proportional to the amount of stress relaxation. τ_1 and τ_2 govern the early and late relaxation responses respectively.

Using this approach, the QLV theory has been utilized to model the canine MCL [114]. Based on separate curve fitting $\sigma^e(\varepsilon)$and G(t) to the loading and relaxation portions of the static stress relaxation curve respectively, the constants of the QLV theory were obtained. These constants were then employed to successfully predict the peak and valley stress values of a cyclic stress relaxation experiment. It should be noted, however, that the theory has been developed based on the assumption of an idealized step-change in strain, which is impossible to apply experimentally. Therefore, significant errors could occur when determining the viscoelastic constants, especially τ_1 [27, 42].

Previous methods to account for these errors include, normalization procedures, iterative techniques, extrapolation and deconvolution, as well as directly fitting the measured strain history [19, 26, 42, 61, 80, 82]. Recently, our research center has developed an alternative approach whereby the QLV theory can be applied to experiments which utilize a slow strain rate in order to avoid experimental errors such as overshoot and vibrations [3]. Using Boltzmann's superposition principle, it can be shown that the loading portion of a stress relaxation experiment with a linear strain history and strain rate, γ, for $0<t<t_0$ can be described by:

$$\sigma(t) = \frac{AB\gamma}{1 + C\ln(\tau_2/\tau_1)} \times \int_0^t \left\{1 + C(E_1[(t-\tau)/\tau_2]E_1[(t-\tau)/\tau_1])\right\} \times e^{B\gamma t}\partial\tau + D(t) \quad \textbf{(4)}$$

Where $D(t) = G(t) + k$.

Similarly, the subsequent stress relaxation at a constant strain from t_0 to $t = \infty$ can be described by changing the upper limit of integration in Eq. (4) from t to t_0:

$$\sigma(t) = \frac{AB\gamma}{1 + C\ln(\tau_2/\tau_1)} \times \int_0^{t_0} \left\{1 + C(E_1[(t-\tau)/\tau_2]E_1[(t-\tau)/\tau_1])\right\} \times e^{B\gamma t}\partial\tau \quad \textbf{(5)}$$

where A, B C, τ_1, and τ_2 are material constants to be determined. Simultaneously curve-fitting these equations to the loading and relaxation portions of the data from a stress relaxation experiment and assuming ligaments are relatively insensitive to strain rate allows the constants A, B, C, τ_1, and τ_2 to be determined [3]. Because this approach accounts for relaxation manifested during loading, the errors in the obtained constants resulting from the assumption of an idealized step-elongation are minimized.

While various investigators have noted experimentally that the viscoelastic behavior of ligaments is largely non-linear meaning the amount of relaxation or creep is dependent not only on time but strain level [17, 47, 93], QLV theory assumes that the relaxation response is strain

level independent. However, the constants still allow for comparisons between groups where the strain level is the same.

2.3 MCL INJURIES AND TREATMENT

In the United States there are nearly 100,000 cases of isolated MCL (medial collateral ligament) tears plus nearly 50,000 combined MCL + ACL (anterior cruciate ligament) injuries annually [76]. The most common injury mechanism is a severe valgus force produced by a direct blow to the lateral aspect of the leg or by landing on the leg in an abnormal way [29, 32, 43].

Isolated MCL injuries heal with conservative treatment, and the long-term structural properties return to normal; however, the ligament quality, signified by histomorphological appearance, biochemical, mechanical, and viscoelastic properties of the healing tissue remains poor [18, 21, 37, 70, 108, 109, 116]. Physical therapy regimens vary depending upon the seriousness of the injury. The goal of these treatments is to return the patient to full activity once the strength, agility, and propreoception of the injured leg equal that of the contralateral leg. However, the most important factor in returning a patient to normal activity is pain. Treatment techniques include: progressive weight-bearing, range-of-motion exercises, agility, strengthening, and propreoception drills, bracing, and functional electrical stimulation [29, 43].

This non-surgical aggressive rehabilitation treatment of MCL injuries has not always been widely accepted. Prior to the 1980s, clinical management was usually surgical repair followed by joint immobilization as advocated by O'Donoguhue [87]. Later trials and basic-science studies reported equally good results for operative or non-operative treatment for

complete tears [32, 54]. Ellasser et al. also reported that with conservative motion and exercise athletes were able to return to normal activity levels as early as 3-8 weeks post-injury [31]. These clinical trials, as well as many basic-science animal studies from our research center [44, 56, 118], indicate a consensus regarding conservative treatment for isolated MCL tears.

Unlike isolated MCL injuries, clinical management of MCL injuries sustained in conjunction with injuries to other knee ligaments such as the ACL and/or posterior cruciate ligament (PCL) is disputed. Current rehabilitation protocols contain long periods of immobilization [5, 28, 29, 122]. This could be helpful to ACL graft incorporation, assisting tendon to bone healing [95]; however, prolonged immobilization increases the chance of arthrofibrosis and has a negative effect on ligament healing. In addition, the loss of ACL function is detrimental to the healing of an MCL injury [120] because the MCL and ACL jointly stabilize varus-valgus knee laxity [55].

This then raises the question in the case of a combined injury: Is there an optimal treatment? While ACL reconstruction after a combined injury does improve MCL healing compared to no reconstruction, the resulting healing MCL tissue is still inferior to the healing tissue in an isolated MCL injury [90]. Furthermore, clinical and laboratory studies have shown that primary repair of the MCL has no long-term effect on outcome [98, 121]. Therefore, if functional tissue engineering provides a technique in which MCL healing is enhanced it could be applied in the case of a combined MCL + ACL injury, resulting in better patient outcome. The first step towards this goal is to show that application of SIS does in fact improve MCL healing after a clinically relevant injury.

2.4 MCL HEALING AND TISSUE HOMEOSTASIS

The healing process following a tear of the MCL can be roughly divided into three overlapping phases [35, 88, 108]. The inflammatory phase is marked by hematoma formation, which starts immediately after injury and lasts for a few weeks [109]. After 3-5 days, fibroblasts proliferate and produce a matrix of proteoglycan and collagen (especially Type III collagen) to bridge the torn ends. During the reparative phase, over the next 6 weeks, the matrix (predominantly type I collagen) becomes increasingly organized and cellular proliferation occurs [109]. Finally, the remodeling phase, marked by alignment of collagen fibers and collagen matrix maturation, continues for years after the injury [35, 109].

The biochemical constituents of the healing ligament are abnormal even after one year [108]. The MCL healing tissue contains an increased amount of proteoglycans, a higher ratio of Type V to Type I collagen, a decrease in the number of mature collagen crosslinks, fibrils with homogenously small diameters (~70 nm) [83, 99], and the cell alignment is highly disorganized compared to normal [37].

These changes are reflected in the structural properties of the healing FMTC, which are inferior to controls at 12 weeks after injury [108]. By 52 weeks post-injury, the stiffness of the injured FMTC recovered to pre-injury levels, but the varus–valgus (V–V) rotation of the knee remained elevated and the ultimate load of the FMTC remained lower than those of the sham operated MCL [56, 70, 89]. At the same time, the cross sectional area of the healing ligament measured as much as 2.5 times its normal size by 52 weeks [90]. Thus, the recovery of the stiffness of the FMTC is largely the result of tissue hypertrophy.

As a result of the hypertrophy, the mechanical properties of the healing MCL midsubstance remain consistently inferior to those of the normal ligament and do not improve up

to one year post-injury [90, 108]. In terms of the viscoelastic properties of the healing MCL, there is increased viscous behavior, reflected by a greater amount of stress relaxation, for the first 3 months after injury. Some studies suggested that these values returned to normal levels after this time period [21], though others suggested they remained increased [81].

Some literature suggests a tie between the structure and biochemical constituents of tissue and its viscoelastic properties; for example, ligaments with higher water content demonstrated greater cyclic load relaxation [22]. It is also known that glycosaminoglycans have a hydrophilic nature and can attract water molecules into the matrix; thus, the elevated levels of proteoglycans with GAG side chains found in healing tissue [66] can affect the visoelastic properties of the tissue [7, 30, 97]. As well, studies have shown that healing MCL tissue has significantly altered constants describing the QLV theory compared to normal [4, 6]. SIS has shown an effect on gene expression of some small proteoglycans, namely decorin [66]. A denser collagen matrix could affect the viscoelasticty of the tissue [103]. Healing tissue is typically less dense and less organized than normal, and these findings could help explain the differences between viscoelastic properties in healing and normal tissue. As SIS has an effect on the structure and biochemical constituents of the neo ligament, in depth analysis of its viscoelastic properties warranted.

The time-and-history dependent viscoelastic behavior modeled by QLV parameters were also investigated for the healing MCL. In a goat model, it was found that after 12 weeks of healing stress relaxation was significantly higher for the healing tissue compared to normal. The healing tissue also had significantly different QLV parameters AxB, C, and τ_2 [4].

Even without injury, connective tissue is highly dynamic. Studies show a highly non-linear relationship between different levels of stress and ligament properties that can be summed up in Figure 7. The normal range of physiological activities is represented by the middle of the

curve. Immobilization results in a rapid reduction in tissue properties and mass. In contrast, long-term exercise resulted in a slight increase in mechanical properties as compared with those observed in normal physiological activities [109].

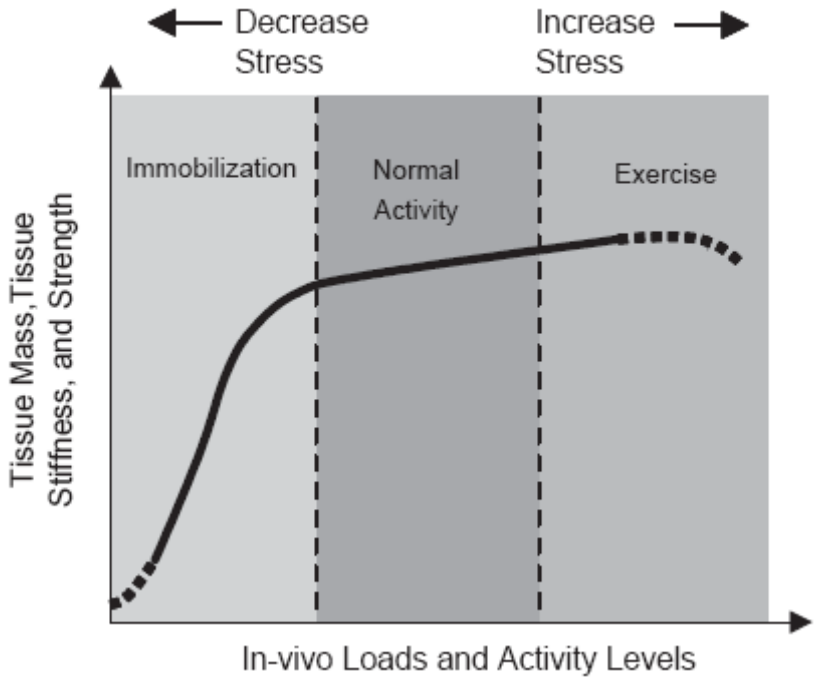

Figure 7. A schematic representing the response of connective tissue to various levels of stress and motion [116].

2.5 INJURY MODEL

When a severe valgus force causes an injury to the MCL, there is damage to the ligament insertion sites, a stress upon the collagen fibers and frayed ligament endings. Researchers have tried many ways to reproduce this injury in animal models with some success. In order to demonstrate the effect of SIS, the injury model used in this study must have the following characteristics:

1. Injury to the insertion sites
2. Over stretching of the collagen fibrils
3. Frayed appearance at torn ends
4. Repeatable injury

Previous investigators have also had the aim to reproduce a clinically relevant injury using various methodologies. Initially investigators have ruptured manually abducted the knee [46, 57, 64, 75]. While this is likely the most clinically relevant way to cause an injury, it is largely inconsistent. In one study, injury location varied many injuries occurring close to both insertions, while some were described as "oblique tears" leaving two long triangular tongues [57, 106]. This inconstancy is troublesome, from a healing stand point. Frank et al. showed that injury location effects MCL healing with, injuries occurring closer to either insertion site healing more slowly than those injured in the midsubstance [37]. In addition to the non repeatable nature of manual abduction, actually producing the injury is quite difficult and requires a great deal of force.

A more controlled method would be to cut the ligament using a scalpel or hemostat [44, 79, 91, 106]. While this is certainly repeatable, it fails to cause injury to the insertion sites, or have a frayed appearance. Histology reveals some mild uncrimping of the collagen fibers near the cut line.

In an effort to have the clinical relevance of the knee abduction and the repeatability of the scapel cut, Walsh et al. compared an injury caused by a scalpel cut to one created by a wire suture rupture morphologically [106]. The wire rupture model creates more damage than the scapel cut, but there is still no visible damage to the insertion site when inspecting morphologically and histologically. However, there was damage done to the small attachments of the meniscus to the MCL with the wire method. The authors concluded that while the wire

method was an improvement over a scapel cut, the damage was still not extensive enough to be "clinically relevant." Therefore they recommended other injury models be found which cause greater damage to insertion sites.

Damage to the insertion site is paramount in a clinically relevant model. It is known that healing of the tissue midsubstance and insertion sites is asyncronys as is evident from failure mechanism, and histologic evidence of osteoclastic bone resorption [108, 116]. Still other studies show that if there is injury to the insertion site, healing of the whole complex can be delayed [57, 75].

Figure 8, a schematic from Weiss et. al. 1991, illustrates the strength of the tibial insertion site as a factor contributing to the changes in the ultimate load and stiffness characteristics of the healing FMTC. Just after injury the strength of the insertion sites is compromised. Then, because of lack of stress, the insertion sites begin to remodel and properties decrease until the two ruptured ends join. This allows for stress to return to the entire complex, and both the insertion sites and midsubstance remodel, signified by an increase in the structural properties [108].

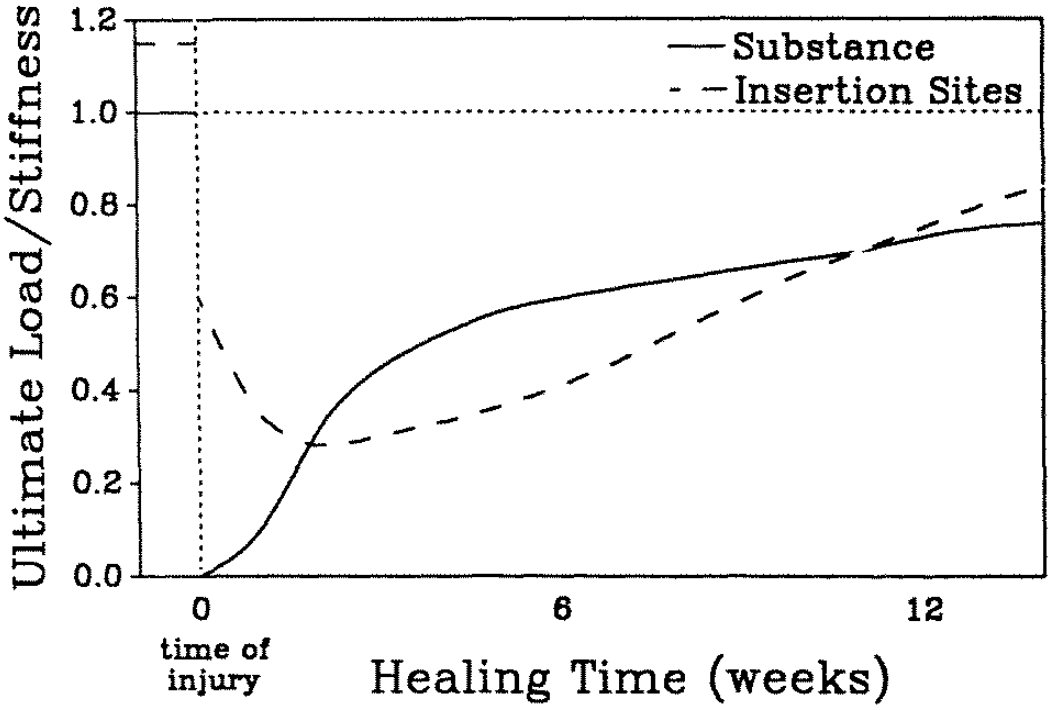

Figure 8. A schematic of the changes to the structural properties of an MCL and the insertion sites [108].

To fulfill the need for a repetable injury with damage to the insertion sites, over streaching of the collagen fibers and frayed ligament ends, a mop-end tear injury model was developed in our laboratory by clinician S. Horibe [108]. By pulling medially on a rod underneath an exposed MCL, the ligament ruptured in tension, producing a midsubstance tear with simultaneous damage to the ligament insertion sites. The ends of the ligament were frayed, and frequently broken into several discrete bundles, giving a mop like appearance (Figure 9). Later histological evaluation confirmed injury to the insertion sites [108]. With this methodology, a consistent injury can be obtained, while still being clinically relevant, thus this injury model has been utilized in this thesis.

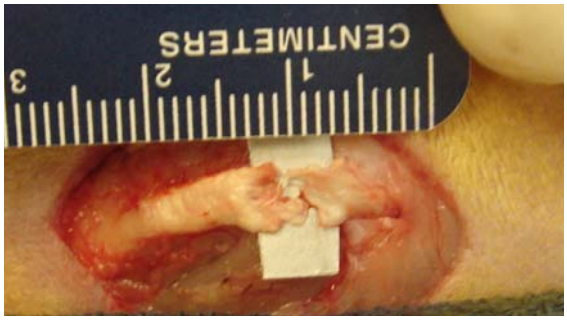

Figure 9. MCL just after mop-end tear.

2.6 FUNCTIONAL TISSUE ENGINEERING

In order to improve the quality of healing tissues where natural healing is limited or conventional/surgical treatments result in impaired joint function, other approaches were investigated. Functional tissue engineering provides attractive tools, which not only aim at restoring the macro- and micro-structures of injured ligaments/tendons, but also the normal joint function. Examples include the usage of a variety of growth factors, gene therapy, cell therapy, and the use of scaffolding materials [109]. While all of these methods show promise and warrant study, growth factors, gene therapy, and cell therapy have challenges for implementation in the human body such as safety concerns (gene therapy) or logistics (cell therapy), which makes scaffolding a favorable choice for translatable research.

2.6.1 Scaffolds.

Generally, scaffolding materials serve as guides for cells to migrate, proliferate and synthesize new extracellular matrices, as well as provide mechanical support during repair of injured tissue. Scaffolds are either synthetic or naturally occurring, and both of these scaffold types have

strengths and weaknesses. Production and design of synthetic scaffold characteristics like pore size, alignment, degradation rate, and bioactivity can easily be controlled. However, the design of synthetic scaffolds often mimics the charactersitcs of bioscaffolds like alignment, optimal pore size, and growth factor bioactivity, which are optimized already for use in the body. Because naturally derived scaffolds, are built by the body to organize cells, including acellular dermis, amniotic membrane tissue, small intestine submucosa, fascia, and acellular bladder matrix [48], it is logical to use them for FTE applications.

2.6.2 Small Intestine Submucosa.

Small intestine submucosa (SIS), is particularly desirable for this study because it has demonstrated promising results in both laboratory and clinical settings in enhancing tendon and ligament healing [11, 13, 14, 23, 25, 38, 59, 60, 67, 92]. SIS possesses a structural hierarchy that is naturally arranged with the ECM proteins collagen Type I with collagen Types III, IV, V, VI, and VII. In addition, SIS contains fibronectin, glycoaminoglycans, hyaluronic acid, chondroitin sulfates A and B, heparin, heparin sulfate and cytokines such as TGF-β1, BFGF, VEGF, and so on [10, 50, 51, 53, 68, 74, 105]. Further, the immune-mediated inflammatory reactions evoked by SIS are limited due to the processing of the scaffold and the actual chemical makeup of the scaffold itself [8, 9, 49, 52].

These intrinsic properties have made the use of SIS attractive for clinical settings. As of 2004, over 250,000 patients have been implanted with SIS, for ailments involving general surgery, gastroenterology, and urology, with largely positive results [11, 12, 38, 62, 72, 86, 102]. In addition to the clinical success, SIS may be ideal for application to ligaments and tendons because it can act as a guide for the cells to grow on in an organized manner and it contains

growth factors which chemoattractants which increase cell migration to the injury site and elicit a favorable gene expression from these cells (i.e., down regulation of Types III and V collagen).

2.7 THE USE OF SIS IN RABBIT MCL WITH 6 MM GAP INJURY

Our research center has completed a few studies concering SIS and the biomechanics of the healing MCL. A 6 mm gap injury was created in the MCL of many rabbits, half were treated with SIS and the others left non treated. After 12 and 26 weeks of healing the animals were euthanized. At both time points Hematoxylin and eosin (H&E) staining showed that the collagen fibers for the SIS-treated group stained denser and were more aligned along the longitudinal axis of the ligament. The 12-week slides are seen in Figure 11. Also, there were more spindle–shaped cells in the SIS-treated neo-ligament. Transmission electron microscopy (TEM) demonstrated that larger collagen fibrils started to appear as early as 12 weeks post-injury, with increasing numbers at 26 weeks. The collagen content, examined with a hydroxyproline assay, demonstrated that SIS could increase the collagen deposited, which was 36% higher compared to the non-treated group at 12 weeks post-injury. Moreover, the collagen type V/I ratio, measured by SDS-PAGE, was 5-6% lower than the non-treated group ($p < 0.05$).

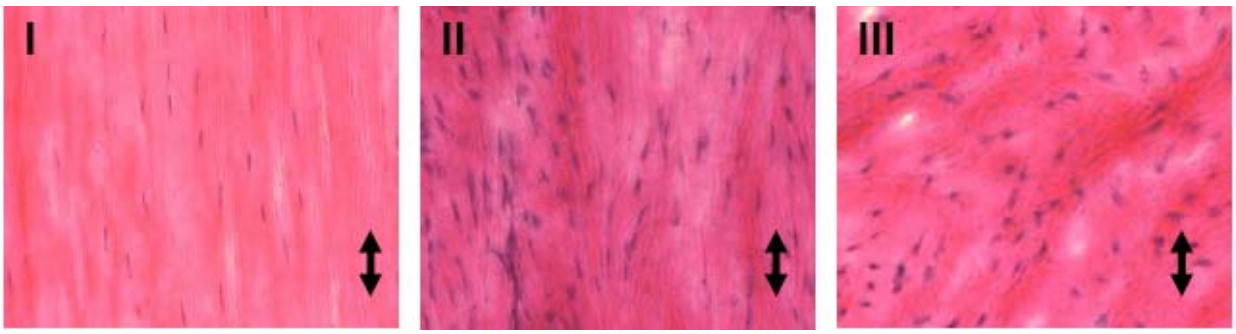

Figure 10. H&E staining of MCL. I Sham tissue; II SIS-treated healing tissue; III NT healing tissue 12 weeks post-injury. The arrows denote preferred direction, adapted from [67].

Corresponding to these structural and biochemical changes, mechanical properties of the healing MCL treated with SIS showed significant increases compared to the non-treated group. Specifically, the tangent modulus of the healing MCL was 50% higher with SIS treatment at 12 weeks, and persisted up to 26 weeks (33% higher; $p < 0.05$) (Figure 11). The tensile strength at 26 weeks post-injury was also 49% higher ($p < 0.05$). Since SIS has been shown to be feasible in a severe transection injury it is important to show its efficacy in a clinically relevant model.

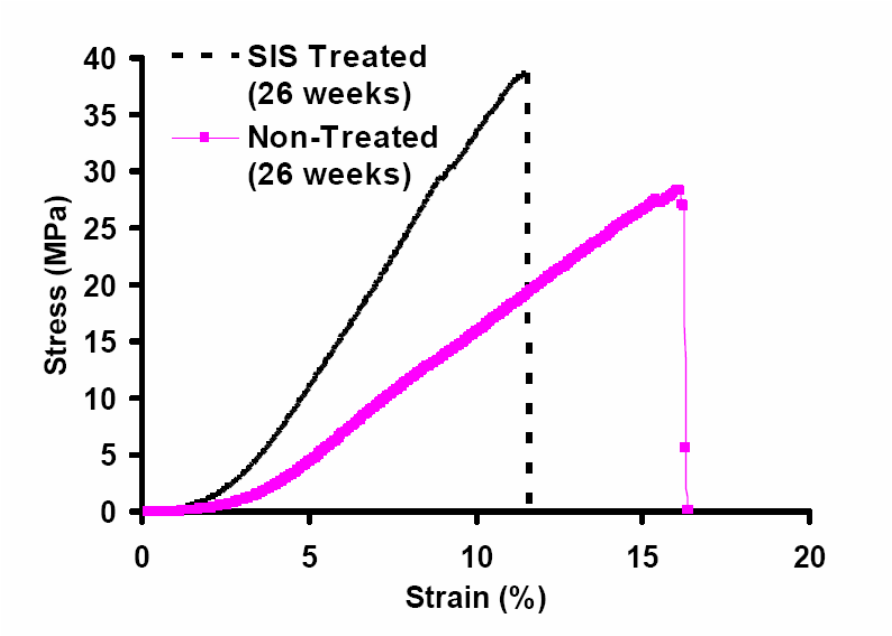

Figure 11. Typical stress-strain curves for SIS-treated and non-treated groups at 26 weeks post-surgery [67].

For the rabbit, the healing tissue was also statistically different in terms of QLV parameters, specifically A, AxB, C and τ_1 [6]. However, significant changes between SIS and non-treatment were only seen for AxB (or the initial slope). These findings, as well as the structural and biochemical changes seen between SIS and NT, suggest that a more in-depth analysis is necessary to fully understand the healing of the MCL in the presence of SIS.

3.0 OBJECTIVES

As the feasibility of SIS to improve MCL healing has been demonstrated with a 6 mm gap injury, the **objective of this thesis was to improve the outcome of ligament healing after a more clinically relevant injury by applying SIS to the injury site.** To fulfill this objective, **i**mprovement in the structural properties of the FMTC and mechanical properties of the tissue midsubstance and its time-and-history dependent viscoelastic properties will be examined. Improvement will be qualitatively assessed through the examination of the gross morphology and histology of the healing tissue.

To answer the research question, **Is there a role for SIS to improve MCL healing in a realistic injury model at 12 weeks?** The following specific aims will be studied:

Specific Aim 1: To assess the positive effects of SIS in the restoration of a ligament's quasi-static biomechanical properties after an injury to the tissue mid-substance and insertion sites.
It has been shown that SIS can increase the collagen fibril diameter and improve the collagen-fiber alignment of the healing MCL, thus improving the midsubstance's mechanical properties [67, 79]. However, those studies were performed using controlled injury models with no injury to insertion sites.

Hypothesis 1: Due to chemoattractant properties and contact guidance [105, 107], SIS treatment will accelerate the healing of the MCL tissue [67, 79], allowing for faster transmission of load across the bone-ligament-bone complex which has been shown to improve the resulting tissue quality [45, 56, 115, 118]. Thus, given both the inherent qualities of the SIS and a more severe

mechanical environment, the histomorphological appearance and biomechanical properties of the SIS-treated ligament will more closely resemble those found in normal MCLs as compared to non-treated controls.

Specific Aim 2: Describe the effect of SIS treatement on the viscoelastic behavior of the rabbit healing ligament using an existing phenomenological model.

Previous studies have shown that healing MCL tissue is significantly more non-linear and has higher amounts of stress relaxation when compared to sham controls [3, 71, 79]. Similarly, when the healing MCL tissue is analytically described using an existing constitutive model based on quasi-linear viscoelastic (QLV) theory, both the instantaneous elastic response and reduced relaxation function constants change [1, 4].

Hypothesis 2: Because SIS has been shown to improve collagen fiber alignment in healing tissue, and fiber recruitment and uncrimping are mechanisms that have been used to explain the non-linear behavior in the "toe region" of the MCL, the use of SIS will result in a non-linear stress strain curve closer to that of the sham control than NT. In addition, the more aligned SIS-treated tissue will have less stress relaxation than non-treated tissue.

4.0 METHODS

4.1 STUDY DESIGN

To accomplish these specific aims, an animal study was conducted using 16 New Zealand white rabbits. This number was determined using a power analysis, estimating a power of 0.8, a significance value of 0.05, and an effect size of 50%. Citing the 12-week gap injury model having SIS improve over NT 50%, and using generous standard deviation estimates, a power analysis revealed that seven specimens per group were needed to detect a difference of 50% in the tangent modulus. Thus, the 16 rabbits were allocated seven per group for biomechanical testing and 2 per group for histology. Two additional rabbits were purchased in case of premature death.

4.2 SURGICAL PROCEDURES

Nine animals per treatment group (7/grp biomechanics, 2/grp histology) will be given an intramuscular (IM) preanesthetic dose of xylazine HCl 0.1 mg/kg and ketamine HCl (3.3 mg/kg), and a preoperative antimicrobial dose of 20-25 mg/kg Cephazolin. The fur will be shaved from the hind limbs, and the exposed area will be sterilized with betadine solution.

An isolated MCL injury will be created by making an anteromedial incision centered over the joint line and carried down to the deep fascia. The fascia will be incised, exposing the MCL that is to be undermined. In the right knee (experimental), a stainless steel rod (4-mm-diameter for goats; 2-mm-diameter for rabbits) will be passed beneath the ligament, just inferior to the attachment of the medial meniscus, and pulled medially to rupture the ligament [89]. The left knees of all animals will serve as sham-operated controls [96, 108]. Skin incisions for the shams will be the same as for the experimental groups. The fascia over the MCL will be incised, and the MCL will be undermined for all shams.

For SIS-treated MCLs, a sheet of SIS (approximately 200 μm thick) will be punched using a custom-made stamp to a size of 5 mm x 10 mm, and placed in normal 0.9% saline. The strip will then be laid on top of the MCL, centered over the rupture site with the luminal side facing toward the MCL. To assure stable positioning of the SIS and to mark the location, Nr. 6.0 Silk sutures will be used to tie the SIS to the MCL in a single stitch fashion at each of the four corners.

Postoperatively, all animals will be allowed free cage activity (cage area, 0.5 m^2). The status of weight bearing and the general health conditions of all animals will be monitored during recovery. Cephazolin (20-25 mg/kg) will be administered twice a day for five days post-operatively for infection prophylaxis. Xylazine will be injected intramuscularly (0.05-0.3 mg/kg) twice a day for three days postoperatively as an analgesic. A lethal injection of sodium pentobarbital intravenously (50-100 mg/kg) while under sedation will be used to humanely euthanize the animals at the time of sacrifice. This surgical procedure has been approved by the University of Pittsburgh Institutional Animal Care and Use Committee (IACUC).

4.3 EXPERIMENTAL PROCEDURES

4.3.1 Histology.

For qualitative characterization of the SIS scaffolds and the healing MCL tissue, H&E staining will be performed on sections cut on a cryotome. These sections will be mounted on slides, fixed with acetone and stained with H&E. The slides will then be viewed using normal RGB light and polarized light microscopy. Observations will be made as to the tendency of the cells to aggregate, the average number of cells in cell clusters, and the appearance of cells in different locations. ECM density and alignment will also be observed. A similar number and distribution of cells and a similar arrangement of ECM fibers is expected in the SIS-treated ligaments compared to normal.

4.3.2 Cross sectional area measurement.

A laser micrometer was developed in our research center to measure the cross-sectional area of soft tissues without contacting the tissue midsubstance [65, 110]. Following a well-established protocol, the rabbit legs will be dissected to the FMTC. The tibia and femur will be cut 10 cm from the joint line to allow for placement in the laser micrometer clamps. Then the tibial plateau and femoral condyles will be trimmed within 5 mm of the respective insertions of the MCL to allow for an unobstructed line of sight for the laser. The cross sectional area and shape of the MCL will be measured at three locations: (1) at the center of the joint line, (2) just proximal (approx. 2.5 mm) to the femoral insertion, and (3) just distal (approx. 2.5 mm) to the tibial insertion [108]. The three measurements will be averaged, and this average will be used for

calculating Lagrangian stress (force/initial cross sectional area). The accuracy of this system has been determined to be less than 0.1 mm^2.

4.3.3 Uniaxial Tensile Testing.

Using standard procedures from our research center, the FMTCs will be mounted in custom-made clamps following the cross sectional area measurement [108], fixed to an Instron™ (Instron 5565) testing machine, and immersed in a saline bath that is held at a constant 37 ºC. With the MCL unloaded, specimens will be given 15 minutes to reach equilibrium. Afterwards, the specimen will be preloaded to 1 N, and one cycle of preconditioning will be performed to "settle" the clamps. The specimen will be preloaded to 1 N yet again and the gauge length reset. It will then be preconditioned for 10 cycles between 0 and 0.75 mm, which equates to loading within the toe region of the stress-strain curve. This will be followed by 1 hr of recovery; a static stress-relaxation test whereby it will be elongated to 0.75 mm (~ 3% strain) [108] and held for a period of 25 min; 1 h recovery; a cyclic stress-relaxation test whereby it was subjected to 30 cycles of elongation between 0.5 and 0.75 mm;, and finally, a load-to-failure test (Figure 12). All tests will be conducted at an elongation rate of 10 mm/min, which corresponded to a strain rate of 0.457 %/s. A Motion Analysis™ video tracking system will be used to track markers on the surface of the ligament (1 cm apart) and centered about the joint line.

Structural properties of the FMTC (i.e., stiffness, ultimate load to failure, elongation to failure, and energy absorbed) and mechanical properties of the ligament substance (i.e., elastic modulus, stress at failure, strain at failure, and strain energy density) will be determined from the resulting load-elongation curves and stress-strain curves, respectively [108]. The data from the static and cyclic stress relaxation tests will be modeled using QLV theory [3, 4, 41]. The values

of the parameters determined from this model will then be used for statistical comparisons between groups.

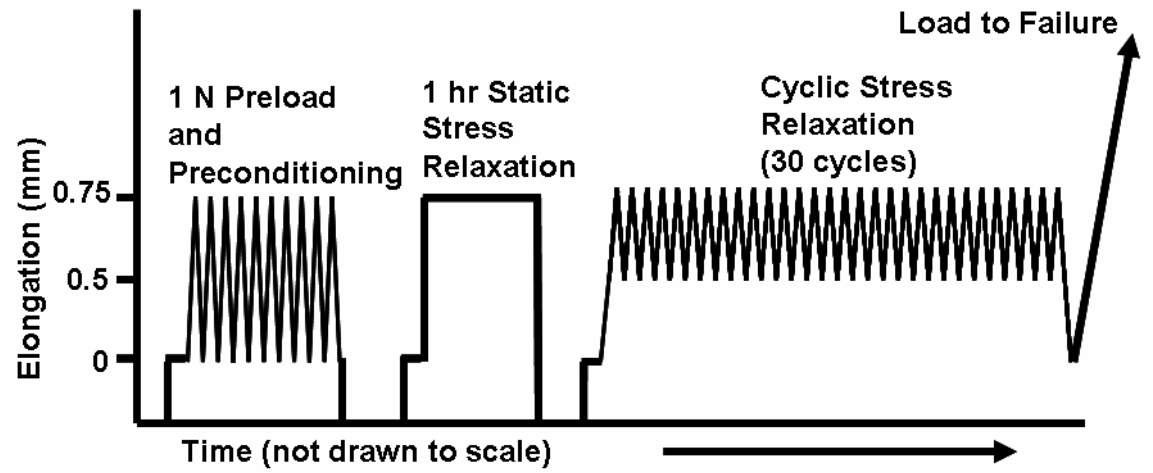

Figure 12. Tensile testing protocol, 1 hour of recovery between tests.

4.4 EXPERIMENTAL PROCEDURES

The QLV theory of Fung [41] will be used to examine the stress relaxation behavior of the normal and healing MCL under uniaxial tension. This theory has been used previously by our research center to describe the viscoelastic properties of the injured and uninjured MCL and PT [2, 6, 34]. A description of the theory can be found in Section 2.2. In order to find 5 physically significant constants (A, B, C, τ_1, τ_2) the ramping and relaxation phases of the experimental stress relaxation data will be simultaneously fit using an algorithm developed by our research center [3] to obtain a unique solution with parameters describing the viscoelastic properties of the MCL. This approach has also recently been modified to account for an initial preload applied to tissues during tensile testing experiments [34].

4.5 STATISTICAL METHODS

In order to compare mechanical and structural properties (e.g. elastic modulus, tensile strength, etc.) between treatment groups (SIS vs. NT), an unpaired *t*-test will be performed. If the experimental treatment group is significantly different from the non-treatment group, then paired *t*-tests will be utilized to compare the experimental treatment group to the contralateral sham-operated control.

When comparing the QLV parameters between groups, it will first be necessary to determine if the experimental data and obtained constants from individual specimens were normally distributed. For this, a Kolmogrov-Smirnov test will be used. If it is normally distributed, a student-t test will be used to compare constants between SIS-treated and non-treated groups. The experimental groups will be compared with the sham-operated control groups by using a paired t-test. The significance level for all comparisons will be set at $p < 0{:}05$ [4, 6].

5.0 RESULTS

5.1 GROSS INSPECTION

During dissection, it was noted that all of the mop-end injuries healed with neoligamentous tissue. All specimens healed with continuity, except for one in the SIS treated group (specimen # 183-06). This specimen had a small defect in the tissue near the femoral insertion, which was covered by a thin film of tissue. With the exception of this specimen, the SIS group had a more uniform, dense midsubstance than the NT group. In both treatment groups, there was hypertrophy of the tissue mass compared to measurements made at surgery, as the ligaments generally lengthened and widened.

There was a reddish tint to most of the healing ligaments, especially near either insertion site. For the SIS group, the tissue between the suture markers near joint level was white in color and mostly opaque, but not as organized as the sham. After failure, the femoral insertion was inspected and a brownish hard cartilage-like tissue was seen in a number of specimens in both treatment groups. For the sham-operated side, gross inspection revealed no significant swelling or inflammation. Figure 14 below shows a typical gross view of the FMTC for each treatment group, as well as the sham-operated group.

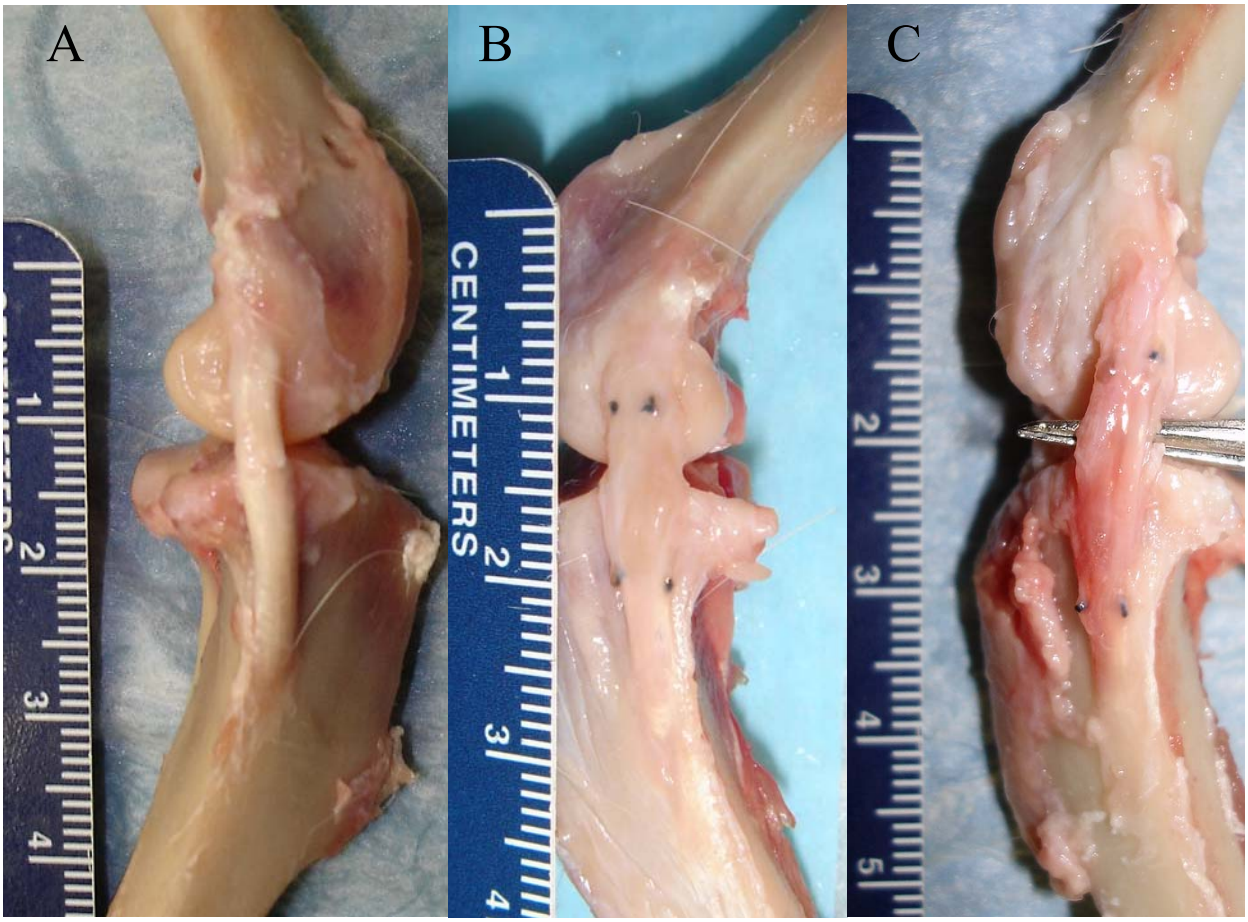

Figure 13. Gross morphology of FMTC of (A) Sham tissue; (B) SIS treated; (C) Non-treated.

There was one specimen, in the SIS treated group #183-06 where the healing response was vastly different than all other healing specimens, let alone those in the SIS treated group. Figure 14 shows the gross morphology of the tissue. Important to note is the near-transparent thinning near the femoral insertion. It is here that the ligament failed during the load-to-failure test. While the odd healing response was noted during dissection, it was only the second specimen to be tested, thus the "normal" gross morphology of the SIS-treated healing tissue was not yet known. It was therefore tensile tested and showed the lowest structural and mechanical properties of all healing specimens tested. The test results confirmed that the specimen was abnormal; its stiffness was nearly 1/3rd smaller than the average of the SIS-treated group (21.2

N/mm), whereas its ultimate load was an order of magnitude smaller than the average (31.4 N). The tangent modulus was an abysmal 71.5 MPa, only 20% of the average of the SIS group.

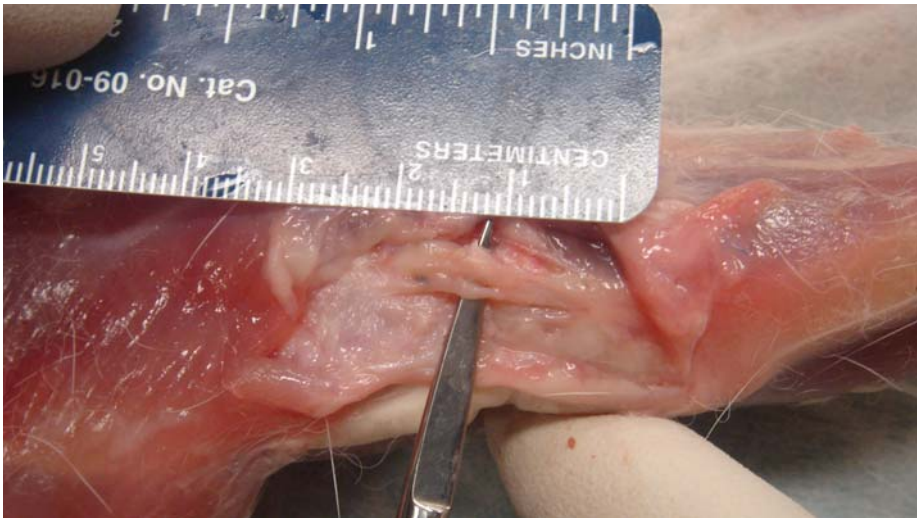

Figure 14. Gross morphology of specimen # 183-06 during dissection; note the discontinuity in the healing tissue.

While it is not documented, there is a strong possibility that this rabbit's adverse healing response was a result of infection, reopening of the wound, sickness, or any number of other confounders. Even though the reason has not been discovered, it is clear that this was abnormal response and thus will be excluded from the remainder of the results.

5.2 HISTOLOGY

Figure 15 shows an H&E staining 200x of both treatment groups. This and other histological evaluation clearly showed there was a difference in matrix density between the two groups, with the SIS group having more tightly packed collagen fibers at 12 weeks. In addition, the ECM was

more organized and had a higher cell count. Cell shape in both groups was elongated and spindle shaped.

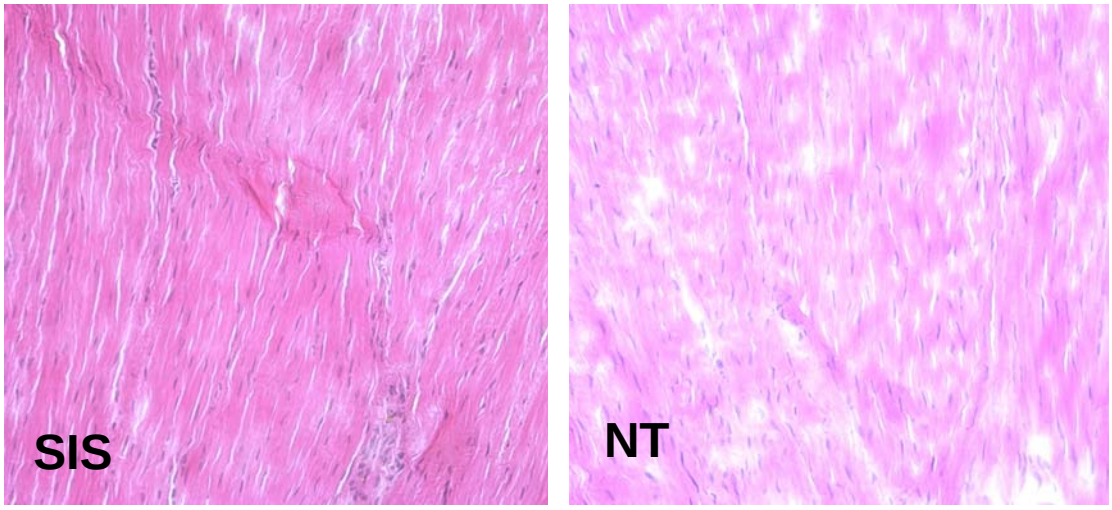

Figure 15 H&E staining at 200x of SIS and NT healing tissue.

Polarized light microscopy confirmed that the new ECM of the SIS-treated ligaments was dense. It also revealed more organized collagen fibers in the SIS group. Fiber crimp was not noted in either treatment group. Figure 16 shows both polarized and normally lit histologic sections at 100x for both treatment groups.

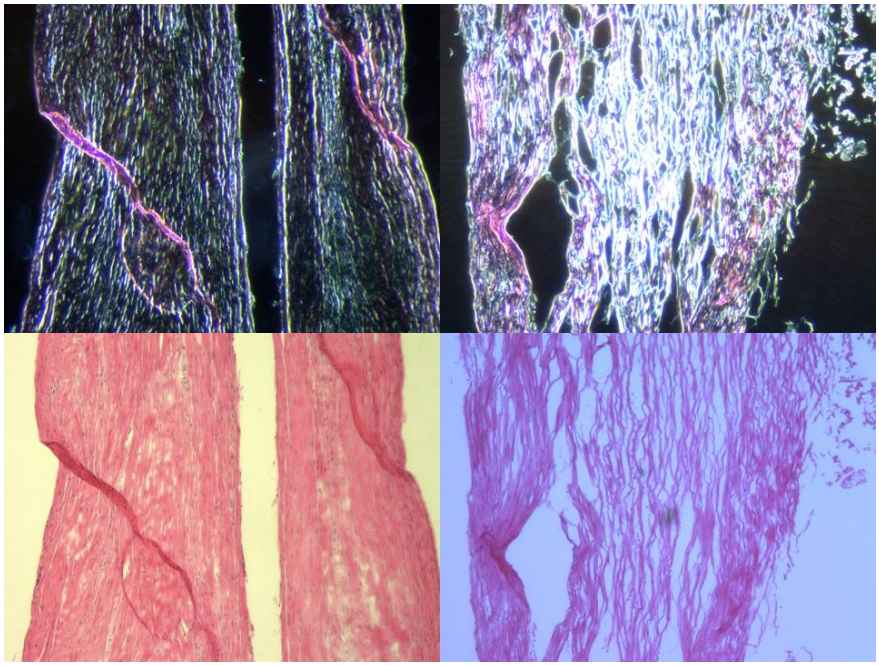

Figure 16 H & E staining at 100x of SIS and NT healing tissue viewed with polarized and normal lighting.

5.3 CROSS SECTIONAL AREA

There was no statistical difference between the cross sectional area of the treatment groups (SIS-treated 7.2 $\pm$ 1.1 and NT 7.3 $\pm$ 2.1 mm); however, both were about twice as large as the sham-operated side (3.6 $\pm$ 0.7 mm^2, $p<0.05$). None of the healing specimens exhibited any major concavities.

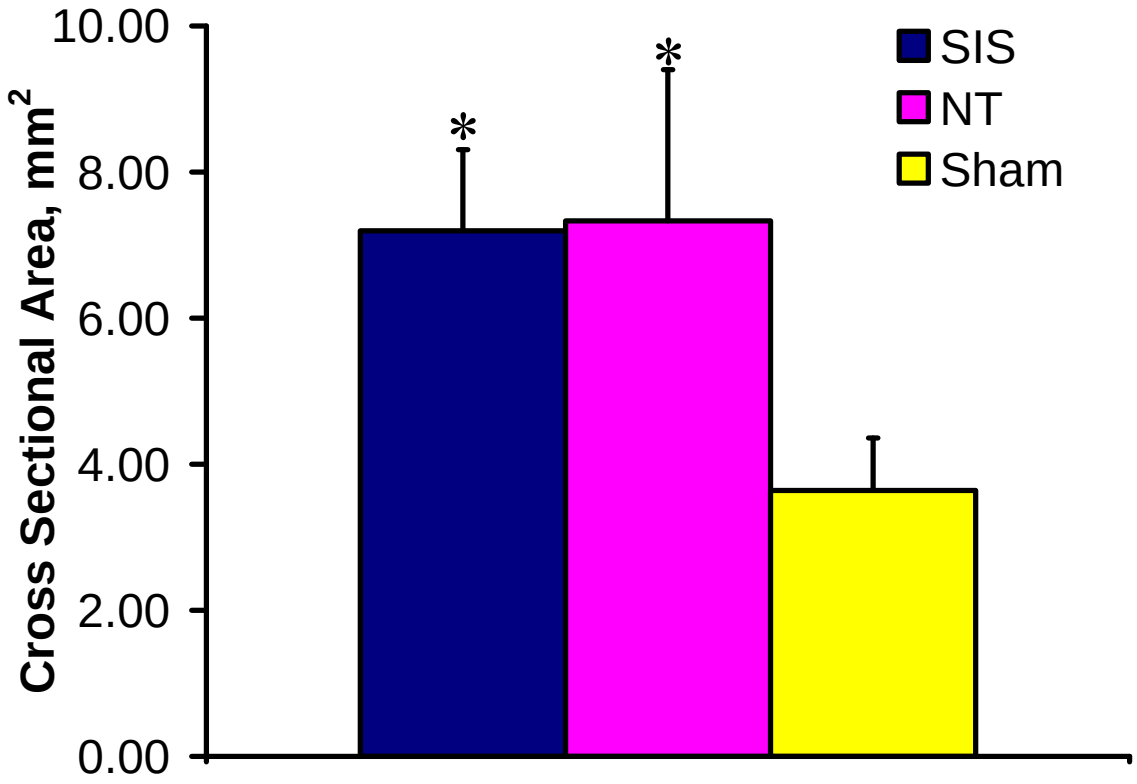

Figure 17. Cross sectional area of the three groups, * denotes significant difference from sham.

In all the healing specimens, the largest of the three CSA measured was near the femoral attachment, slightly above joint level (close to where the ligament was injured). Starting from the measurement at the femoral insertion and moving distally toward the tibial insertion, the CSA of these healing groups reduced. The CSA of the SIS-treated group decreased 1.6 mm^2 and

0.9 mm^2 from the proximal to joint level and joint level to distal, respectively, whereas in the NT group the CSA was reduced 2.0 mm^2 from the proximal to joint level, and 0.3 mm^2 from the joint level to the distal measurement point. The CSA of the sham-operated control was relatively consistent along the length of the ligament with a decrease of 0.5 mm^2 from the proximal to joint level and a decrease in CSA of 0.1 mm^2 from the joint level to distal. At all three levels of measurement there was no statistical difference between treatment groups, while both were statically different from the sham control. Figure 18 shows a CSA values for the treatment groups at the three measurement levels.

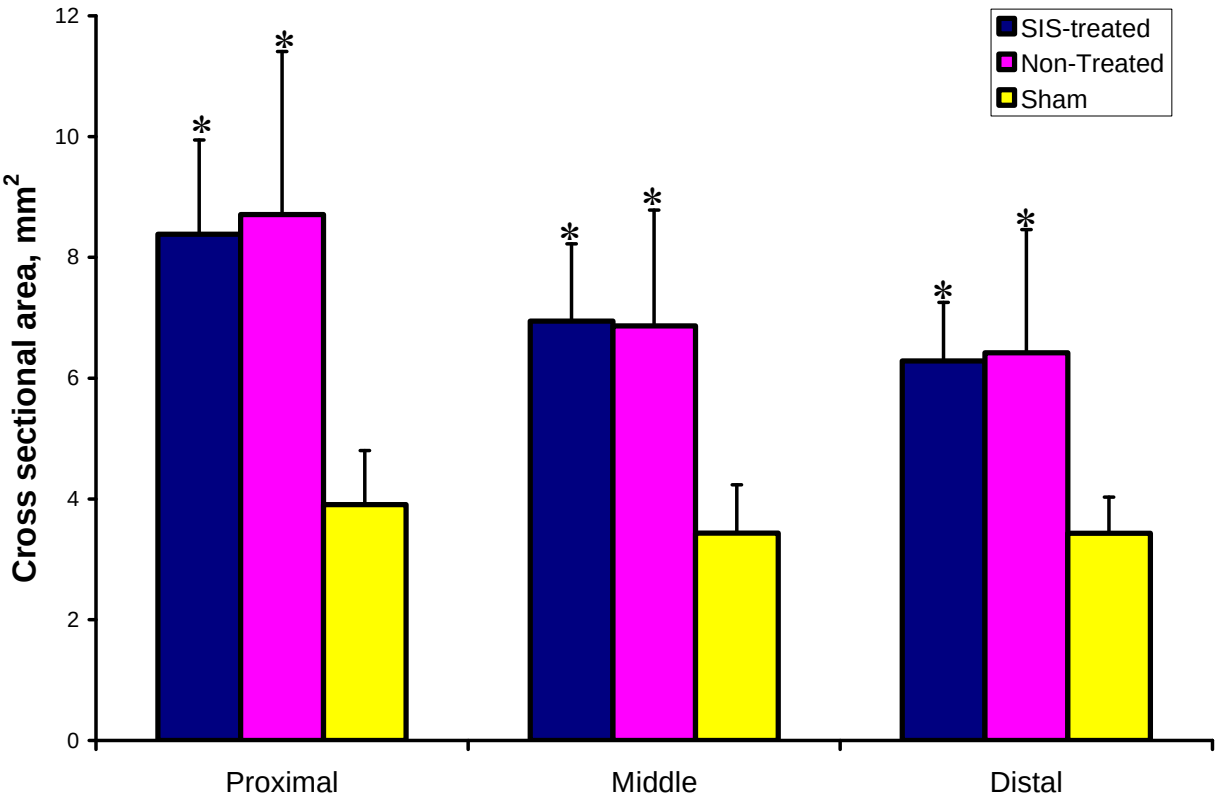

Figure 18. Cross sectional area of the three groups compared at different measurement levels.

5.4 STRUCTURAL PROPERTIES

Structurally, no statistical difference was found between the two treatment groups. This is demonstrated by the typical load elongation curves shown in Figure 19. Both groups exhibited a non-linear toe region for the first 0.5 mm of elongation. After this, the bone-ligament-bone complex of both treatment groups exhibited a linear relationship between elongation and load. The average values of the parameters describing this load elongation curve (stiffness, ultimate load, elongation at failure and energy absorbed) are listed in Table 1. The stiffness of the SIS-treated group was

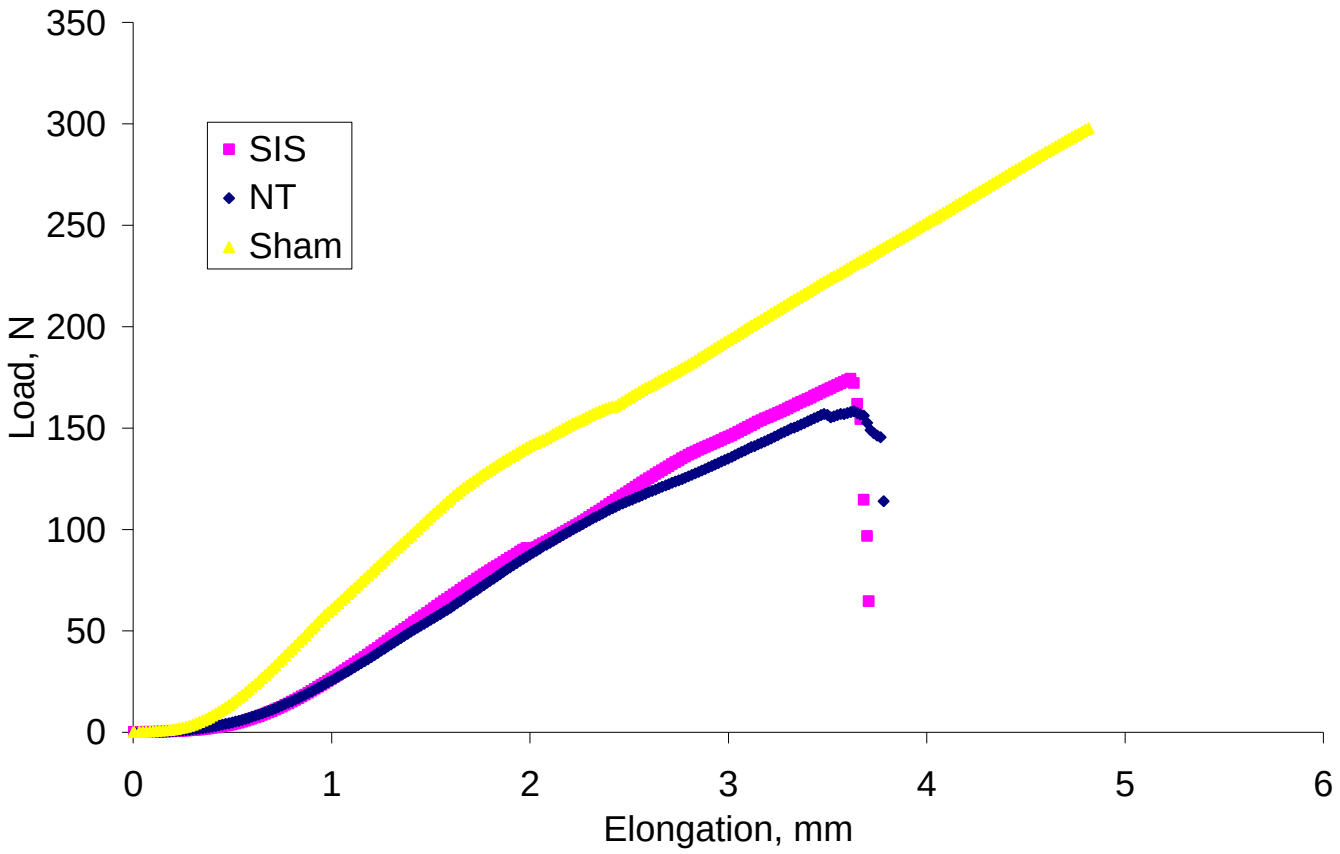

Figure 19. Typical load-elongation curves for SIS, NT, and Sham groups.

larger than the non-treated group, though not significantly (SIS 63.8 ± 9.4 N/mm vs. 56.8 ± 8.6 N/mm, $p < 0.05$). The ultimate load and energy absorbed, too, were larger in the SIS group, but not significantly.

Both groups are significantly less than the sham-operated control. Stiffness of the SIS group being ~75% of the sham control, and the NT group being ~63% of control. The ultimate load in both healing groups was restored ~55% and ~44% of sham for the SIS and NT groups, respectively. The ultimate elongation for both healing groups was 70% of sham.

Table 1. Structural properties of the FMTC, a denotes significant difference from sham ($p<0.05$)

	SIS (n=6)	**NT (n=7)**	**Sham (n=13)**
CSA, mm^2	7.2 ± 1.1[a]	7.4 ± 2.1[a]	3.6 ± 0.7
Stiffness, *N/mm*	63.8 ± 9.4[a]	56.8 ± 8.6[a]	88.7 ± 10.0
Ult. Load, *N*	145.6 ± 57.2[a]	137.7 ± 45.9[a]	283.9 ± 40.7
Elongation at Failure, *mm*	3.1 ± 0.9[a]	3.3 ± 0.9[a]	4.6 ± 0.5
Energy Absorbed, *N*mm*	226 ± 149[a]	211 ± 145[a]	685 ± 155

Failure mode was classified in three categories: midsubstance failure, failure in the ligament stubstance near the tibial insertion, and tibial insertion site failure. (The difference between tibial insertion site failure and failure in the ligament substance near the tibial insertion is, in the case of that a tibial insertion site failure, the ligament completely shears off the face of the tibia, whereas a failure in the ligament substance leaves some ligament on the bone. In both instances, stress estimation is not valid.) In the SIS-treated group, three failed in the mid-substance and three failed at the tibial insertion site. The NT group had zero midsubstance failures, four in the ligament substance near the tibial insertion, and three failed at the tibial insertion. Therefore, almost half of the 13 experimental specimens failed at the tibial insertion

site, meaning the insertion site was the area most prone to failure. Eight of the sham-operated control group failed in the midsubstance. Five of the 13 sham tissues failed by femoral avulsion due to removing too much of the femoral condyles during dissection in order to fit the FMTC into the clamp. Many of the animals were small, and as such, the ligament length between insertion sites was short.

5.5 MECHANICAL PROPERTIES

The mechanical properties of the ligament midsubstance are detailed in Table 2. Typical stress–strain curves of healed FMTCs from SIS-treated and nontreated groups are shown in Fig. 20. As the healing tissues failed in various places, only the tangent modulus of the ligament midsubstance will be compared between groups. The ultimate stress, ultimate strain, and strain energy density could only be found in the three SIS specimens which failed in the midsubstance. The tangent modulus of the healing tissue midsubstance in the SIS-treated group measured ~30% greater than that of the non-treated group, and was significantly larger (403.9 ±119.5 MPa vs. 272.9 ± 90.9 MPa, respectively, $p < 0.05$). Both treatment groups were significantly smaller than the sham-operated control (1180.7 $\pm$ 316.4, $p<0.05$).

Table 2. Mechanical properties of the healing tissue midsubstance, a denotes significant difference from sham, b denotes significant difference between treatment groups ($p<0.05$)

	SIS (n=6)	NT (n=7)	Sham (n=13)
Modulus, *MPa*	403.9 $\pm$ 119.5[a,b]	272.9 $\pm$ 90.9[a,b]	1180.7 $\pm$ 316.4

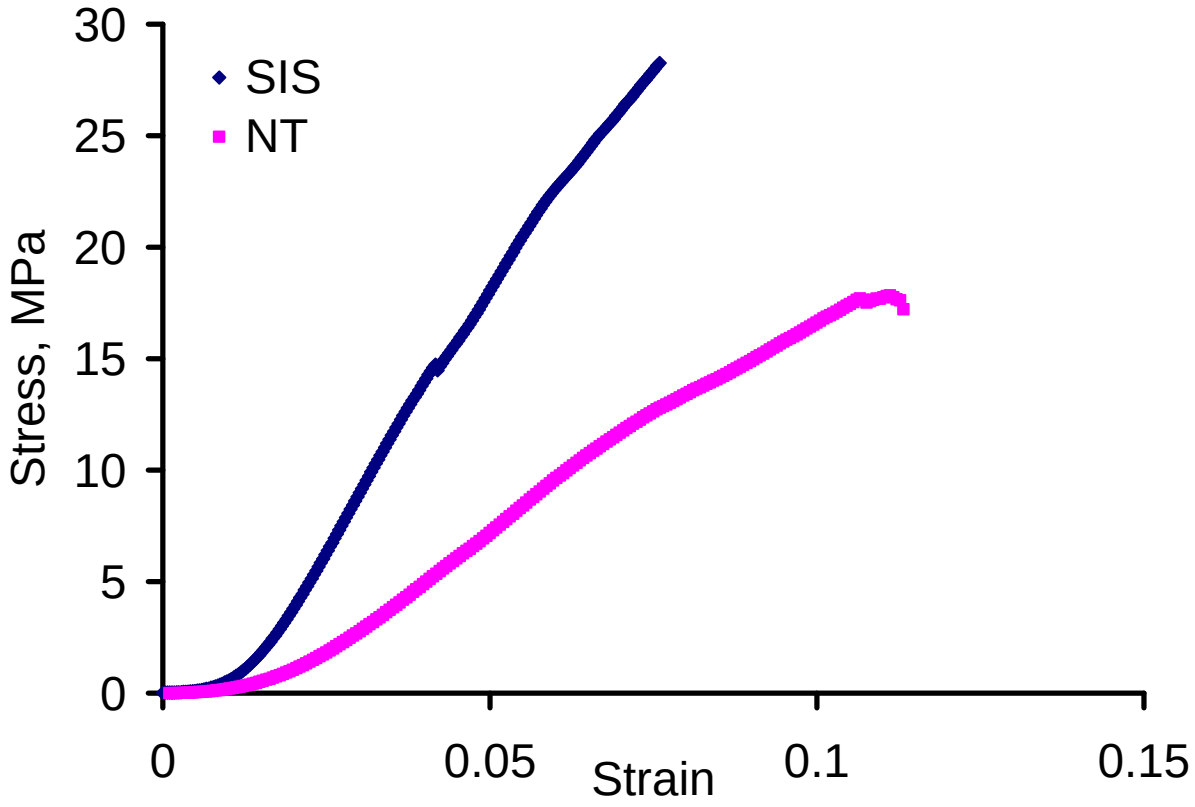

Figure 20. Typical stress-strain curves for the treatment groups.

5.6 VISCOELASTIC PARAMETERS

Investigating the time-dependent behavior of the healing tissue, a static stress relaxation test was used. The peak strains for the static stress-relaxation test were 1.4 + 0.5% and 2.2 + 1.1% with peak stresses of 3.4 + 0.8 and 2.7 + 0.7 MPa, respectively, for the SIS and NT groups. The peak strain was indistinguishable from the Motion Analysis data for two of the six SIS specimens and thus was not included in this data. For all but these two specimens, the average strain rate from the static stress relaxation, cyclic stress relaxation and load-to-failure tests was used as an input for the QLV curve fit. The strain rate from the load-to-failure test was used for these specimens.

At 25 min, the total amount of stress relaxation not found to be statistically different between groups and was to be 54.9 + 7.4% and 58.1 + 6.5%, respectively. Comparing both healing groups to sham (30.7 + 5.7% static stress relaxation), healing tissue generally relaxed 28% more than sham tissue based on the static stress relaxation curves. For the cyclic stress-relaxation tests, the peak stress decreased by 31.3 + 4.2% and 34.7 + 4.6%, respectively, after 30 cycles of elongation. The peak stress, final stress, peak strain and stress relaxation of both groups were all statistically different than sham. Table 3 sums up this behavior, while Figure 20, shows typical stress relaxation curves on both normal and log timescale.

Table 3. Basic viscoelastic behavior of the tested specimens; a denotes significant difference from sham ($p<0.05$).

	SIS (n=6)	NT (n=7)	Sham (n=13)
Static stress relaxation			
Peak Stress, Mpa	3.4 ± 0.8[a]	2.7 ± 0.7[a]	13.1 ± 3.1
Final Stress, Mpa	1.5 ± 0.5[a]	1.2 ± 0.5[a]	8.4 ± 2.5
Peak Strain, %	1.4 ± 0.5	2.2 ± 1.1	2.7 ± 1.2
Percent Relaxation, %	55.4 ± 7.3[a]	58.1 ± 6.5[a]	36.8 ± 10.5
Cyclic stress relaxation			
Percent Relaxation from Cycle 1 to Cycle 30, %	31.3 ± 4.2	34.7 ± 4.6[a]	20.1 ± 7.0

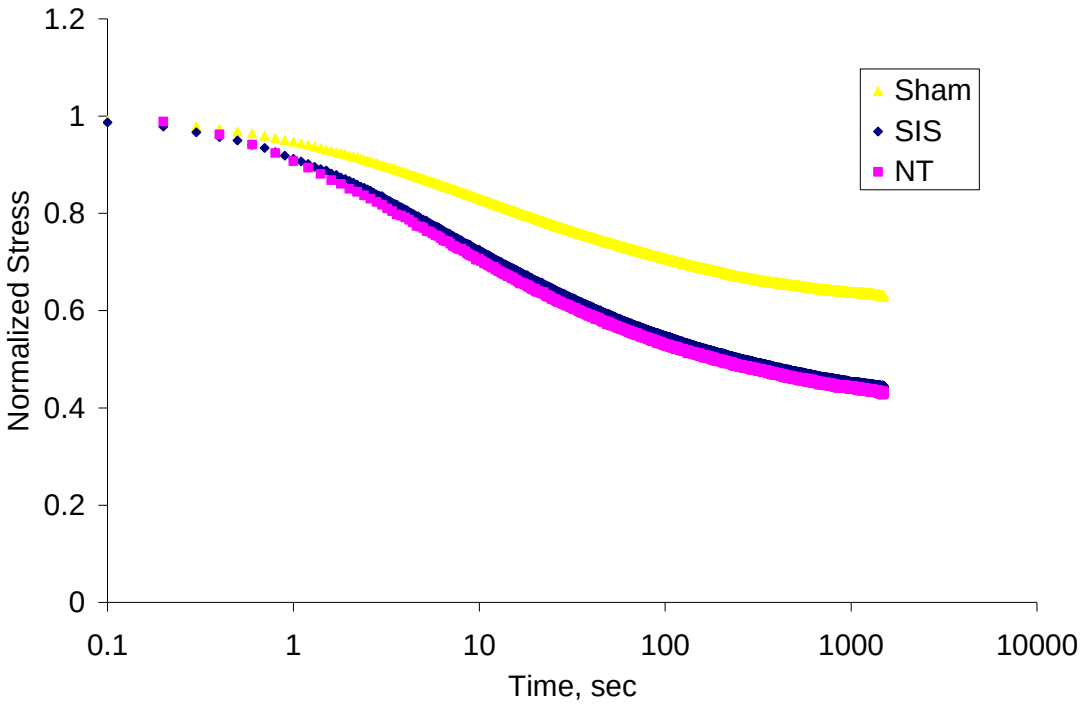

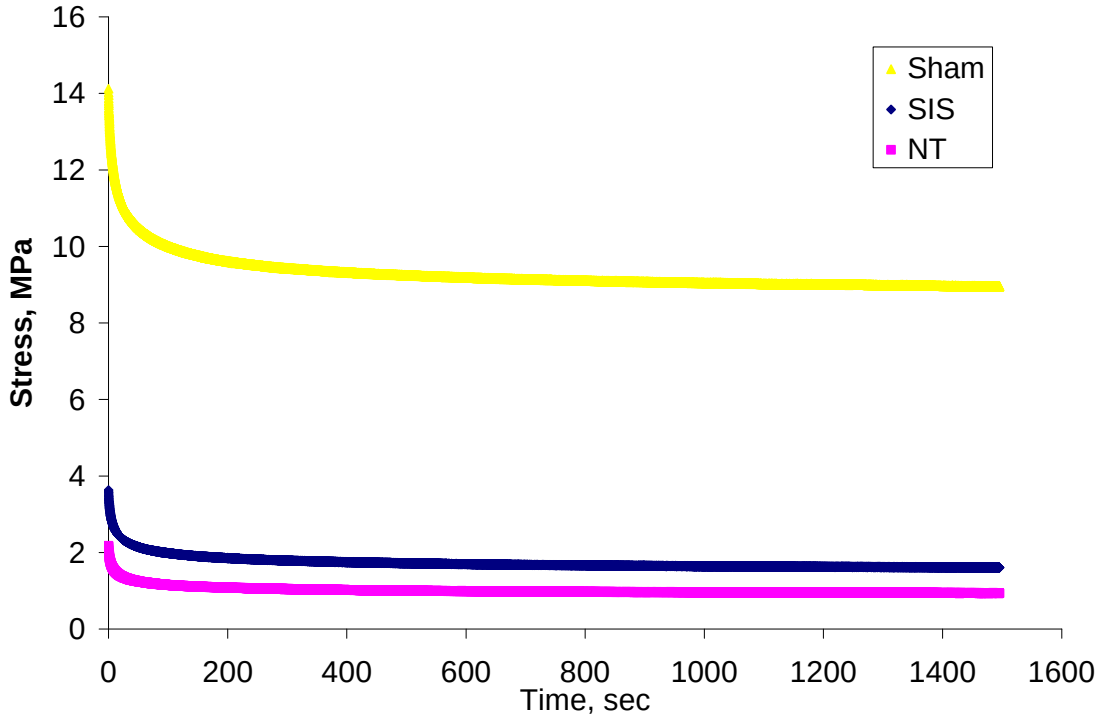

Figure 21. Typical stress relaxation curves on (A) log , and (B) normal time scale.

Curve fits of the static stress relaxation data using the QLV theory revealed an R^2 value of 0.98 or higher for all specimens. All variables were found to be normally distributed therefore a student t-test was used to compare treatment groups. There was no statistical difference found between the treatment groups in any of the QLV constants; however, AxB for the SIS trended to be higher than NT control, meaning that the initial slope of the elastic response function appeared to improve with SIS treatment. To compare the experimental groups to sham controls, a paired-t test was used. Both experimental groups were statistically different from sham controls for A, and AxB. Table 4 displays the means and standard deviations for each parameter in the three groups (SIS, NT, and Sham).

Table 4. QLV parameters of the experimental groups; a denotes significant difference from sham ($p<0.05$).

	SIS (n=6)	NT (n=7)	Sham (n=13)
QLV parameters			
A	1.8 ± 1.3[a]	1.4 ± 0.8[a]	8.5 ± 5.5
B	74.1 ± 24.1	55.4 ± 15.3	57.8 ± 32.3
A x B	115.0 ± 46.1[a]	71.0 ± 15.3[a]	414.24 ± 201.4
C	0.20 ± 0.03[a]	0.22 ± 0.07[a]	0.11 ± 0.06
τ_1	0.13 ± 0.01[a]	0.11 ± 0.02[a]	0.13 ± 0.3
τ_2	665 + 475	501 ± 74	533 ± 112

To validate these constants, experimental peak stresses of the 30 cyclic stress relaxation cycles were compared to predicted values calculated with constants in Table 4 and equations 1-5 (Section 2.2). Generally, the predictions were best for the first few cycles, and the accuracy of the peak stress prediction decreased with each new cycle. The sham-operated control was the most accurate, predicting the peaks within the acceptable 10% accuracy. Surprisingly, the experimental groups were not this accurate. The SIS predictions were as high as 37.1% off from the measured experimental stresses (average error for all specimens all peaks being 22.6%). The

NT group was no better with an average error of 23.0%. Figure 22 compares the predicted and experimental peak stress for each of the SIS and NT groups.

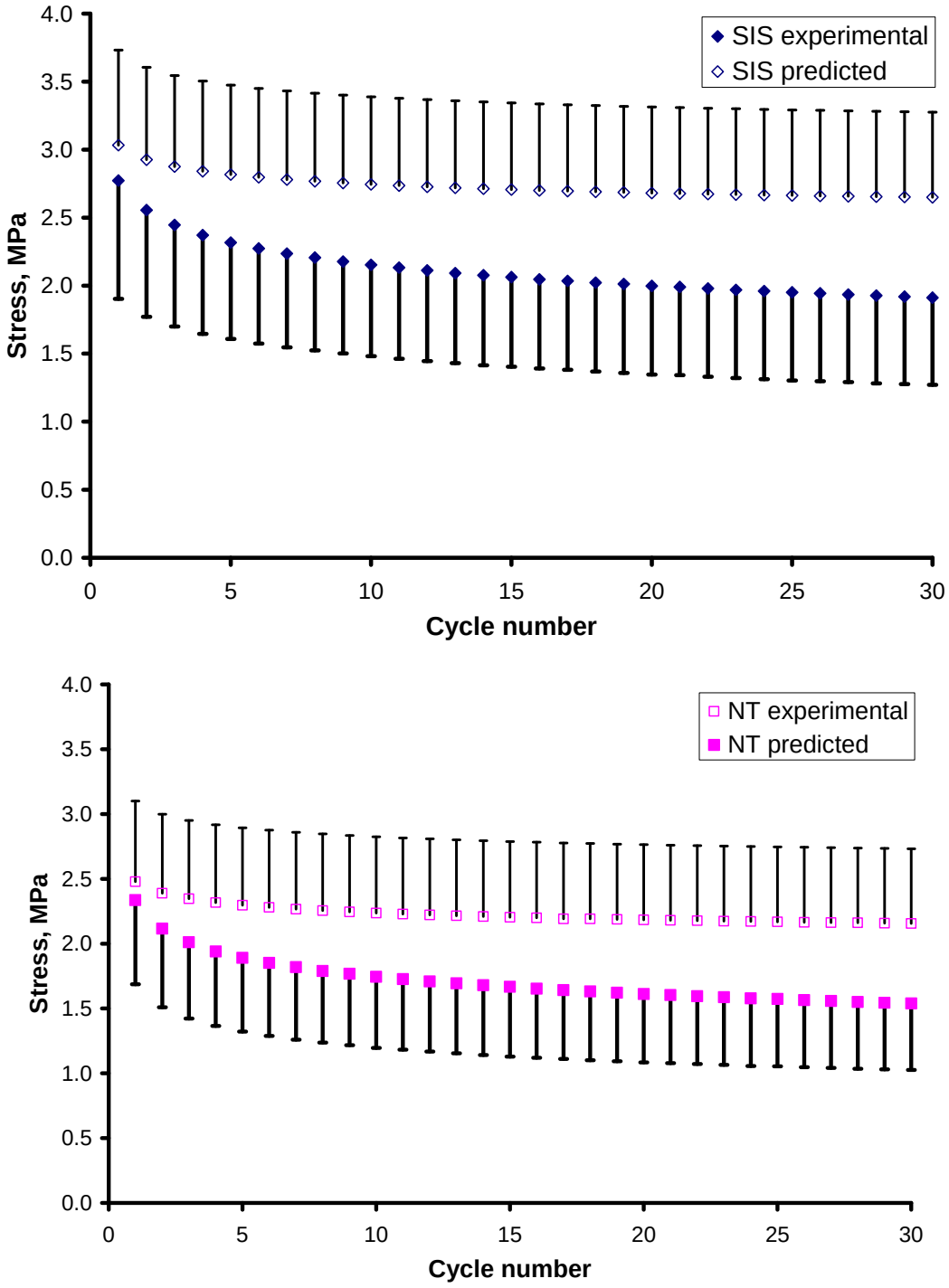

Figure 22. Mean and standard deviations of both the experimental and predicted peak stresses for each of the 30 cyclic stress relaxation cycles.

6.0 DISCUSSION

6.1 HYPOTHESIS 1

Restated, Hypothesis 1 was: Due to chemoattractant properties and contact guidance [105, 107], SIS treatment will accelerate the healing of the MCL tissue [67, 79], allowing for faster transmission of load across the bone-ligament-bone complex, which has been shown to improve the resulting tissue quality [45, 56, 115, 118]. Thus, given both the inherent qualities of the SIS and a more stringent mechanical environment, the histomorphological appearance and biomechanical properties of the SIS-treated ligament will more closely resemble those found in normal MCLs as compared to non-treated controls.

This hypothesis was shown to be partially supported. SIS did improve the inherent quality of the tissue, as is evidenced by a 32% increase in tangent modulus, as well as histological evidence of a more organized matrix; however this did not translate to improved structural properties. Logically, if there is the same amount of higher quality tissue (CSA of the two groups was not different), then there would be an improvement in that tissue's ability to resist load, so why was no improvement in structural properties observed? Looking at failure mode, nearly half of all the experimental group specimens failed at the tibial insertion (3/6 in the SIS and 3/7 in the NT). This was similar to the non-repaired group of the Weiss and Woo study in which 3 of 6 FMTCs failed by tibial avulsion [108], making the insertion site the weakest link in both studies. The Weiss study postulated that insertion site healing and midsubstance healing

are asynchronous, and SIS did nothing to change this. Rather it had a very localized improvement in tissue quality, much like the gap injury studies. A comparison between the mop-end tear study and the gap injury SIS treatment studies offers further support as to why there was no structural property improvement.

6.2 COMPARISON WITH GAP INJURY RESULTS

For this thesis, a single layer of SIS was used to treat a realistic mop-end injury model. This injury model is highlighted by injury to the insertion site of the ligament, frayed edges of the injured ends and stretching of the collagen fibers during injury. SIS treatment saw no statistical increase in CSA or structural properties over non-treatment. However, the modulus of the SIS healed tissue was about 32% higher than the NT healed tissue. This difference was statistically significant. Due to numerous failures at the insertion site for both healing groups (~50 of all the treatment group specimens), other mechanical properties were not compared.

These findings are slightly different from a study conducted with a gap injury to the MCL. At 12 weeks, the stiffness and ultimate load (structural properties) of the FMTC of the two healing groups were statistically different for the gap injury model. SIS improved the stiffness 56%, and the ultimate load nearly doubled compared to NT. Tangent modulus was also statistically different between the two groups. Unlike the gap injury, the mop-end tear causes damage to the insertion sites, this is reflected in the number of insertion site failures. After 12 weeks of healing in this study nearly half of the FMTCs failed at the insertion site, whereas in the gap injury model only 32% of the healing FMTCs failed by tibial avulsion. To confirm that the damage to the insertion site at injury time and the subsequent asynchronous healing of the

insertion site is the reason why SIS did not improve structural properties as well as mechanical properties, a later-timepoint study can be used. Given a longer time span, insertion sites will heal and an improvement in structural properties would be observed.

Another stark difference is that in this thesis, improvement in modulus value was less than that in the gap injury study. The gap injury SIS treatment yielded a tangent modulus over 50% higher than the NT group [79], whereas this thesis only improved the modulus by 32%. And the modulus of the NT group of this study was almost larger than the SIS treated group of the gap injury model as seen in Figure 23.

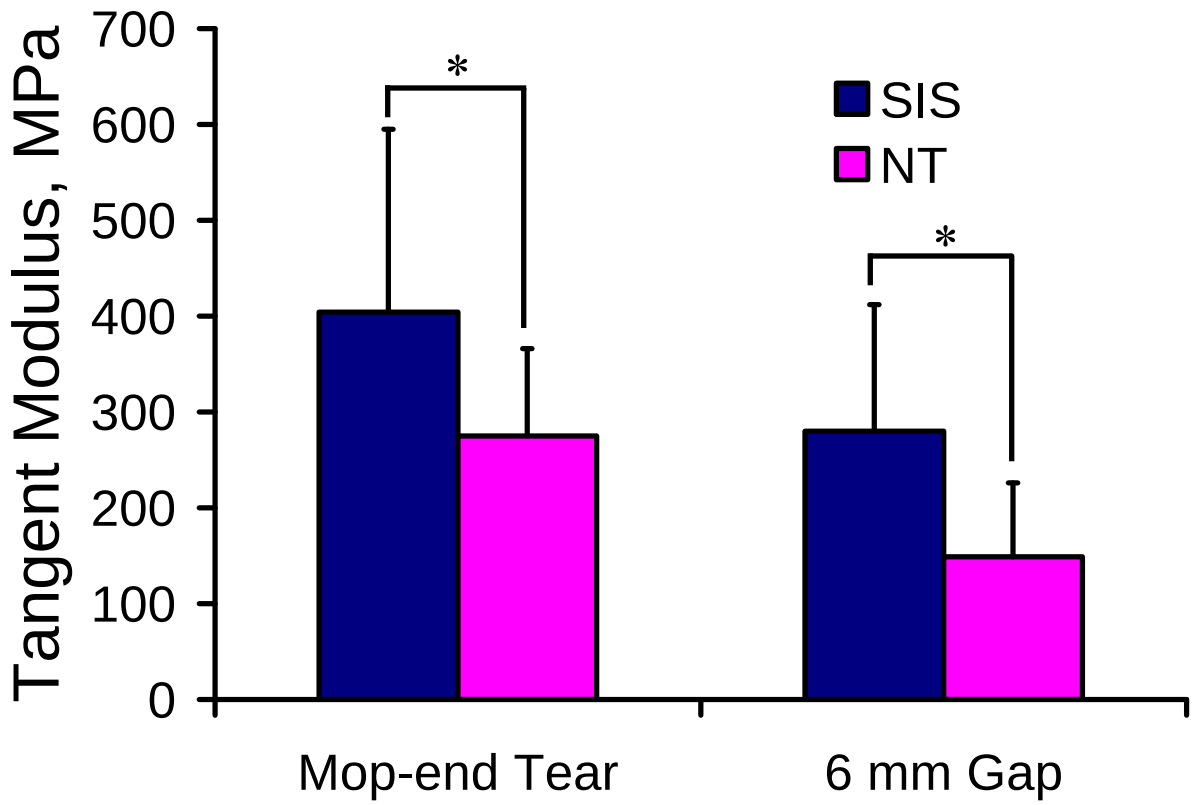

Figure 23. Tangent modulus of both treatment groups for both the mop-end and gap injury models. * denotes significance between groups $p<0.05$.

Gap width could have played a role. Previous studies have shown that as gap width increases the MCL healing response is adversely affected [21, 70]. The gap injury had a

controllable 6 mm gap between injured ends, and in this study the gap between edges at time of rupture was measured to be ~1.6 mm, less than 1/3 of the Musahl et al. study; therefore, the structural and mechanical properties were higher in the mop-end injury. For example, the stiffness in both healing groups for the mop end study was about 60 N/mm, whereas in the gap injury model even with SIS treatment the stiffness was only 45.7 + 13.3 N/mm. Similar trends exist for ultimate load, and modulus. Because the injured ends of the ligament are so close to each other, the non-treatment group has a good start, and SIS may not have as noticeable an effect on the ligament healing. This may explain, in part, why there was no statistical difference in structural properties, and tangent modulus improved only 32% with a mop-end injury while in the gap injury SIS improved it over 50%.

Another possible cause for the difference in results between the two studies is the use of animals from different sources. Even though they were the same species, rabbits in this study were purchased from Covance Rabbitry, while the Musahl et. al. study's rabbits were purchased from Myrtle's Rabbitry. While the animals from the gap injury study were virgin, this study used retired breeders. Also, while the rabbits were the same age, the size of this study's rabbits (4.0 + 0.5 kg) was smaller than those of Musahl et al. (average 5.7 kg).

There were also some slight differences in the mechanical testing protocol. In this study, the preload was only 1 N as compared to 2 N for the gap injury study. Also the preconditioning, static stress relaxation, and cyclic stress relaxation were tested to an elongation rate of 5 mm/min. This change in elongation rate was inconsequential due to the MCL's relative insensitivity to strain rate [119]. Also, the results for the sham control of both studies were similar. Structurally, the stiffness of mop-end and gap injury sham FMTC was 88.5 + 7.5 (n=11) and 89.7 $\pm$ 15.3 (n=16) N/mm, respectively. The ultimate load for either study was 284.2 $\pm$ 42.4 (n=12) and 332.0 + 50.8 (n=16) N, respectively. As far as mechanical properties are concerned,

results again are similar for tangent modulus (sham values for mop-end study: 1086.4 ± 292.9; and gap injury study: 936.3 ± 283.6).

Because the sham data for both studies is reasonably comparable, however, the discrepancy in the effect of SIS on result trends between the studies is therefore likely due to differences in the injury models and not animal source or testing protocol.

Other differences in the injury model may not have had an effect, or at least none that were quantifiable. The frayed edges present in the mop-end tear model likely had little effect, as there have been studies which show that have shown repeatable mop ends created with a scalpel (as opposed to tearing) have little effect on the healing outcome [20]. Regarding the stretching of fibers, while this is a marked difference in the injury models it is difficult to ascertain its effect on the healing response.

6.3 HYPOTHESIS 2

Restated, Hypothesis 2 was: Because SIS has been shown to improve collagen fiber alignment in healing tissue, and fiber recruitment and uncrimping are mechanisms that have been used to explain the non-linear behavior of the "toe region" of the MCL, the use of SIS will result in a non-linearity similar to that of the sham control. In addition, the more aligned SIS-treated tissue will have less stress relaxation than non-treated tissue.

The testing of this hypothesis was inconclusive. None of the QLV parameters exhibited statistical differences between treatment groups. Nor was there a statistical difference in the amount of stress relaxation between groups, in either the static or cyclic stress relaxation test. While the stress relaxation trends had SIS being closer to sham, both experimental groups were

statically different from the sham side. This is consistent with previous data concerning MCL healing and viscoelastic parameters. In the gap-injury study there was no statistical difference found in any of the QLV constants except for AxB [6]. Again, AxB is the initial slope of the elastic response of the tissue; this means that in the toe region of the curve, where strains are in physiologic range, the tissue behaves more like normal. For this thesis, AxB trended closer to sham with SIS treatment, but there was no statistical difference between the two treatment groups. This difference in results could be due to the smaller gap size in the mop end tear injury model. With a smaller gap there is less opportunity for SIS to improve the healing tissue. This is similar to why there was less improvement in tangent modulus in the mop-end model than in the gap-injury model.

A major issue with the QLV constants is their inability to predict the peak stresses during cyclic stress relaxation. In some cases the predicted values were 37% different than the measured experimental values. Looking deeper into the data that the peak stress in the cyclic stress relaxation was on average 20% less than that same specimen's peak stress during the preconditioning and static stress relaxation. All three tests went to the same 0.75 mm elongation level. The data also reveals that at the initial gage length of the cyclic stress relaxation test, the load was near 0 N, while it should be around the preload of 1 N. Next, looking at the strain data for the two tests, the strain rate was the same for most specimens, but the peak strain level was smaller for the cyclic stress relaxation test. Simply put, some slack was systematically introduced to the system between the static and cyclic tests, which needed to be removed before the tissue could be strained; thus, in the 0.75 mm elongation, the tissue was not being strained the whole time in the cyclic test, a lower strain level was achieved, and a lower stress output was recorded.

The constitutive model predicted values of stress based on strain values that were not reached experimentally. Ideally, this would have been noticed and corrected in preliminary testing, as it is a systematic experimental error. However, this can be corrected with some manipulation to the predictive modeling program. The program essentially uses strain rate to determine the amount of strain the tissue is undergoing. It also utilizes a t_0 term and cycle frequency to determine how long the tissue is being strained. It was noticed in the strain data that because of the slack in the tissue, the t_0 terms entered into the predictive program were too large, and the tissue was not strained as much as the model predicted.

To solve this issue, the three specimens that had the largest errors between the prediction and experimental values were used (#s 188-06, 225-06, and 643-06). The load-time data from the static stress relaxation was used to see at what time during loading the peak load from the cyclic test was obtained. This was compared with the cyclic strain data, specifically how long it took to go from zero strain to the first peak strain. The two times were very similar, and less than the amount of time the tissue was strained for the static stress relaxation. So by altering t_0 in the prediction program to accurately reflect the time from zero strain to peak strain during the cyclic stress relaxation, the error between the predicted value and experimental values reduced for the worst three specimens. The error on the first peak modestly reduced from 16% to -15%, while on the 30^{th} peak it was reduced from 35% to an acceptable 6%. The peak stress values predicted by both methods and the experimental stress values for specimen #643-06 are depicted in Figure 24. While not ideal, this methodology shows that in fact the QLV constants are valid and the source of error was experimental, not in the predictive constitutive model or curve fitting.

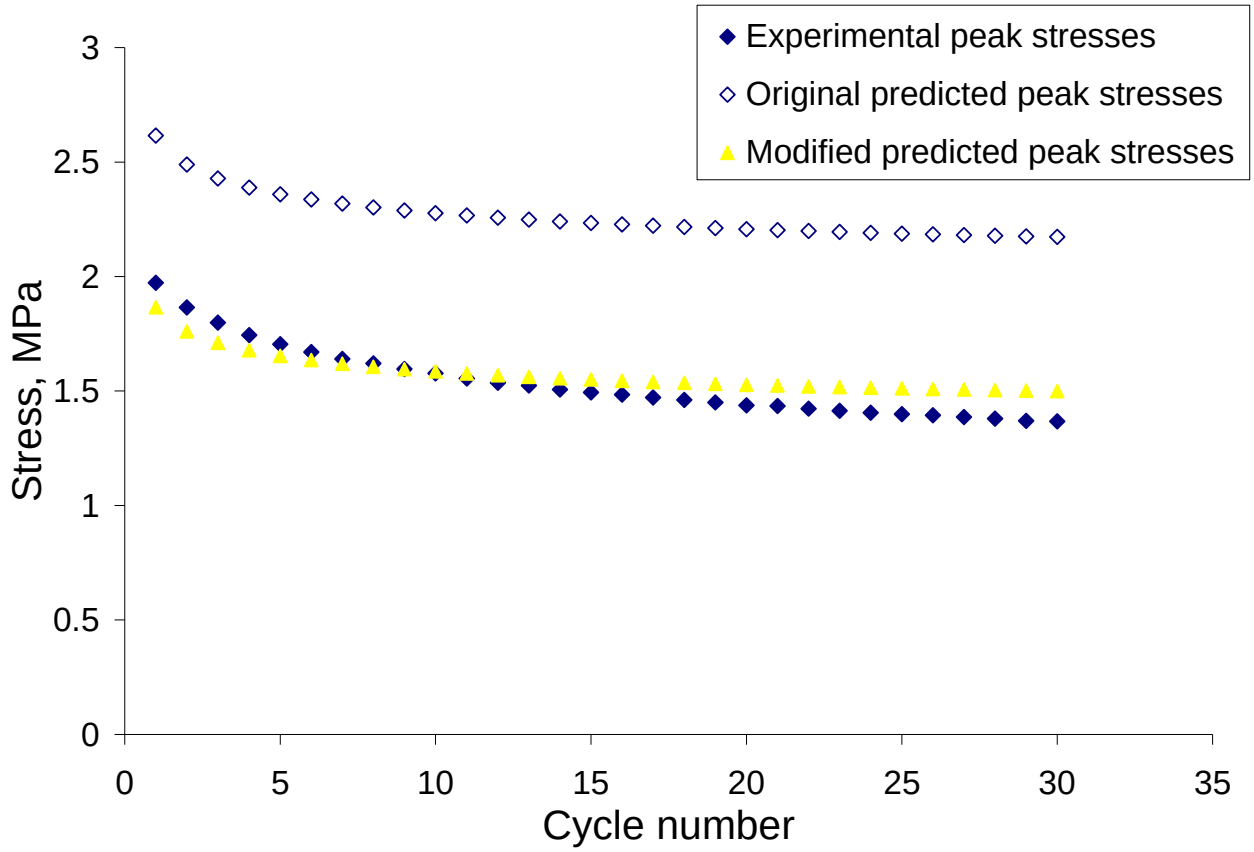

Figure 24. A comparison of the experimental and predicted peak stresses for specimen #225-06, in each of the 30 cycles of the cyclic stress relaxation.

Another interesting result is that the stress relaxation response from the healing and sham tissues was markedly different than previous studies. Comparing the amount of stress relaxation of the sham tissue from the gap injury study (23.8 ± 5.5 %) to this study (37.7 + 10.7 %) a tendency for a higher amount of stress relaxation is revealed. Another study conducted on the rabbit MCL, Moon et al., showed a stress relaxation of 17.2 $\pm$ 4.2 %; again, markedly different than the amount of relaxation seen in this study.

In both of these studies, the elongation level for the static stress relaxation was 1.5 mm, corresponding to 4.2 (Moon) and 5.0 % (gap injury sham) strain [78, 79]. This specimens in this thesis were subjected to half the elongation (0.75 mm), corresponding to 2.7% strain. As such, the ramp time varied between studies from 4.5 seconds (this thesis) to 9 seconds (Moon and gap

injury) [78, 79]. With an increase in ramp time, the tissue was able to relax more before a peak stress was obtained; therefore, with a shorter ramp time more stress relaxation was measured.

This would explain a difference in the amount of stress relaxation however with the current QLV approach taking into account relaxation during the ramp time, and the assumption that the viscoelastic response is strain-level-independent [3], the QLV parameters of the three studies' sham tissue should be similar. Table 5 shows the parameters for each of these studies.

All three studies have a similar AxB, it is important to note that this thesis study has a much larger of B when compared to the other two, meaning the elastic response is more non-linear. This can be explained by the smaller preload (1 N as opposed to 2 N) causing a larger a toe region in the loading data.

The constant C is an order of magnitude larger for this study, signifying a larger amount of stress relaxation, which is the same trend depicted by the % relaxation. However, due to the concurrent curve-fitting of the reduced relaxation function and elastic response, these results should be more similar. There is evidence that the MCL's viscoelastic behavior is not as independent of strain level as once thought. Therefore, the difference in strain level between this thesis and the previous work could explain the discrepancy with the QLV constants[17, 47, 93]. This study had a lower strain level, which theoretically would yield more stress relaxation. This study did have a higher amount of stress relaxation, supporting the nonlinear viscoelastic theory that the MCL is not independent of strain level. However, because we are using QLV theory to compare treatment groups, which have similar strain, levels, its use is still valid.

Table 5. Differences in QLV parameters of normal tissue across various studies

	Moon	Gap-injury	Thesis
	n=6	n=10	n=13
Ramp time	9 sec	9 sec	4.5 sec
Elongation level	1.5 mm	1.5 mm	0.75 mm
A, MPa	12.7 ± 2.5	14.2 ± 4.9	8.5 ± 5.5
B	29.2 ± 1.8	27.1 ± 8.4	57.8 ± 32.3
A*B, MPa	371 ± 78	379.6 ± 177.7	414.2 ± 201.4
C	0.042 ± 0.012	0.05 ± 0.02	0.11 ± 0.06
τ_1	0.35 ± 0.02	0.39 ± 0.03	0.13 + 0.03
τ_2	462 ± 116	424 ± 98	533 ± 112
%relax	17.42 ± 4.2%	23.8 ± 5.5%	36.8 ± 10.5%
Strain level	4.2 ± 0.3%	4.9 ± 1.5%	2.7 ± 1.2%
Modulus, MPa	1107 ± 126	936 ± 284	1081 ± 316

As there was little conclusive evidence from this methodology that SIS treatment had an effect on the viscoelastic properties, in order to verify hypothesis 2 a more in-depth analysis is necessary.

6.4 STUDY LIMITATIONS

A major limitation of this study was the use of the rabbit model. First, the rabbit's knee is always in deep flexion, making its use quite different from a human. In addition, while it is a mammal, the rabbit's healing response is different than a human's. The early phase of healing in a rabbit uses a different type of cell--a heterophil, as opposed to the neutrophil which is present in humans [101]. This, however, is a more conservative model, meaning if there is no adverse response to SIS treatment in the rabbit, then it is almost certain that there would be no rejection from a human.

Group size was also small in this study. Other healing studies have used more animals per group, such as the gap injury studies, which used 8 rabbits per treatment group. Power analysis shows that it would likely take five more animals per group to find significant differences between the two treatment groups for the QLV parameter.

The following revisions would improve this study if it were to be performed again. First, the histology portion of the project was poorly planned. The sections cut were not necessarily able to give the best information on fiber density or alignment under normal light, nor fiber crimp under polarized light. The information desired from histology should have been better outlined before frontal sections were chosen. Also, the insertion sites should have been preserved in the histology animals and made into slides. This would have provided more evidence that the insertion sites were still damaged at 12 weeks. And therefore given support to the explanation for why the improvement in tangent modulus was not coupled with an improvement in structural properties. Secondly, a plan for visual outliers should have been established. Instead of mechanically testing specimen #183-06 after noting its flaws, it could have been useful to save the specimen for biochemical or other evaluation in order to determine why there was an abnormal healing response. Finally, the reduction in peak load between the static and cyclic stress relaxation phases of the mechanical testing protocol should have been dealt with experimentally instead of in the data analysis phase. The reason for this reduction should have been pinpointed before any testing of specimens continued.

7.0 CONCLUSIONS

The research question of this thesis was: **Is there a role for SIS to improve MCL healing in a realistic injury model at 12 weeks?** The results of this study definitively answer this question yes. With improvement in the tangent modulus it is clear that SIS enhances healing of the MCL midsubstance. However, this improvement did not translate to improved structural properties, even though there was a similar amount of healing tissue between the two groups. This is likely indicative of the asynchronous healing of the injured insertion site and ligament midsubstance. Therefore in future studies insertion site healing cannot be ignored. Due to inconclusive results the role of SIS in the healing MCL's vicoelastic properties still needs to be elucidated through other methodologies.

This study also offers information on scaffold design. Some researchers argue that at time zero the scaffold must have the same properties as the native tissue. This study shows that not to be the case--both the mechanical (contact guidance) and chemical factors (growth factors, etc.) of SIS help to improve MCL healing. It is not necessary for a bioscaffold to have the native mechanical properties of the tissue, but rather, it must be utilized in an inductive manner rather than as a mechanical substitute.

These results confirm the feasibility of SIS as a ligament and tendon healing enhancement technique. This is the third study from our research center to show improvement in MCL healing with the use of SIS. This cannot be understated: SIS affects the local healing

response of an MCL, and regardless of injury model, SIS can help the MCL heal. This information is significant as future studies begin investigating the in vivo effect of SIS on the injured patellar tendon or ACL.

7.1 FUTURE DIRECTIONS

With three studies successfully showing MCL healing enhancement by using a single layer of SIS, it is quite clear that this FTE technique has promise in other ligament or tendon injury locations. The patellar tendon after graft harvest and ACL after injury are two that directly come to mind. Both have less than favorable natural healing responses. SIS could also be used to treat the MCL after a joint ACL-MCL injury.

SIS alone may not be enough to improve the healing response in these locations. To improve upon the scaffold, FTE techniques should be combined and studied first in vitro, and then in vivo. Examples of possible techniques include, but are not limited to: combining SIS with some sort of cell therapy, applying stretching to further align the scaffold, or adding growth factors.

In addition, this study confirms the complex nature of midsubstance and insertion site healing and demonstrates that the insertion site cannot be ignored after injury. It also may be possible to treat the insertion sites with FTE techniques as well as the midsubstance.

Also, given the results of the analytic analysis of the viscoelastic properties of the healing tissue in each of the treatment groups, a more rigorous attempt may be needed to fully characterize the complex time-and-history dependent nature of the tissue. As such, it is possible that frequency sweep experimental methods or other constitutive models may be necessary.

Finally, the most immediate step for future work would be to investigate healing over longer time spans with this current injury model. As was previously discussed, using this injury model, SIS improved the tangent modulus of the tissue, but not the structural properties of the bone-ligament-bone complex. This was due to the particularly vulnerable tibial insertion site in many of the treatment group FMTCs. After the insertion sites are given more time to heal the structural properties should improve.

APPENDIX A

RAW DATA FOR SPECIFIC AIM 1

A.1 STRUCTURAL PROPERTIES

Table A-1. Structural properties of SIS group.

	Weight	CSA	Stiffness	Ult. Load	Ult. Elong.	En. Abs.
	kg	mm^2	N/mm	N	mm	N-mm
180-06	3.6	7.66	48.07	55.04	1.78	37.48
181-06	3	5.63	56.83	115.36	2.73	139.09
182-06	4	7.15	72.51	193.75	4.10	419.65
183-06	4	7.25	20.65	31.40	2.23	27.30
184-60	4.1	6.17	66.91	174.35	3.62	283.66
225-06	4.7	8.35	70.17	128.15	2.50	124.36
643-06	4.3	8.22	68.26	207.12	3.93	353.06

Table B-2. Structural properties of NT experimental group.

	Weight	CSA	Stiffness	Ult. Load	Ult. Elong.	En. Abs.
	kg	mm^2	N/mm	N	mm	N-mm
179-06	4.1	8.87	62.93	158.27	3.63	269.76
188-06	4.4	9.96	48.78	213.60	5.18	501.23
226-06	4.1	9.43	66.35	166.83	3.30	238.26
542-06	4.4	7.26	54.56	97.44	2.63	107.95
543-06	4	5.55	65.49	124.48	2.75	123.67
544-06	3.5	5.01	43.86	77.05	2.48	81.55
641-06	4.1	5.5	55.85	125.96	2.93	157.66

Table C-3. Structural properties of Sham group

	Weight	CSA	Stiffness	Ult. Load	Ult. Elong.	En. Abs.	Tan. Mod.
	kg	mm^2	N/mm	N	mm	N-mm	MPa
179-06	4.1	2.31	93.41	297.75	4.82	737.37	1695.42
180-06	3.6	3.34	79.29	246.08	3.83	476.67	879.16
181-06	3	3.89	88.76	246.50	4.07	569.14	789.06
182-06	4	2.94	66.38	264.28	4.72	605.23	1427.92
183-06	4	2.92	86.55	269.00	4.47	625.40	807.09
184-60	4.1	3.57	83.78	269.40	4.57	614.68	862.76
188-06	4.4	4.49	77.89	291.51	5.23	768.43	1170.75
225-06	4.7	4.82	99.15	323.05	4.53	737.12	1112.79
226-06	4.1	4.20	86.09	300.68	4.77	727.72	1151.46
542-06	4.4	2.99	101.95	356.70	5.43	1082.02	1538.29
543-06	4	4.37	99.80	343.27	4.57	797.25	1119.99
544-06	3.5	3.82	92.05	218.11	4.92	680.09	797.36
641-06	4.1	3.07	91.02	284.98	4.13	578.34	1674.08
643-06	4.3	3.52	93.62	248.44	4.02	532.28	1130.57

A.2 MECHANICAL PROPERTIES

Table D-4. Tangent Modulus of SIS group.

	Tan. Mod.	Failure
	MPa	Mode
180-06	231.50	Tibial insertion
181-06	539.89	Mid.
182-06	428.30	Mid
183-06	62.47	Mid.
184-60	517.48	Tibial insertion
225-06	400.79	Tibial insertion
643-06	305.48	Mid.

Table E-5. Tangent Modulus of NT group**.**

	Tan. Mod.	Failure
	MPa	Mode
179-06	236.1	Mid. @ tib
188-06	178.308	Mid. @ tib
226-06	319.15	Tibial insert
542-06	252.81	Tibial insertion
543-06	343.74	Mid. @ tib
544-06	165.5478	Tibial insertion
641-06	414.8457	Mid. @ tib

Table F-6. Mechanical properties of Sham group.

	Tan. Mod.	Failure
	MPa	Mode
179-06	1695.4	M. Subst
180-06	879.2	M.Subst
181-06	789.1	F avuls
182-06	1427.9	M.Subst
183-06	807.1	M.Subst
184-60	862.8	F avuls
188-06	1170.7	M. Subst
225-06	1112.8	F avuls
226-06	1151.5	M. Subst
542-06	1538.3	M. Subst
543-06	1120.0	F avuls
544-06	797.4	M. Subst
641-06	1674.1	F avuls
643-06	1130.6	M.Subst

APPENDIX B

RAW DATA FOR SPECIFIC AIM 2

Table G-1. QLV parameters and percent relaxation of SIS group.

	A	B	A*B	C	τ_1	τ_2	%
180-06	0.81	68.96	56.11	0.124	0.118	1565.8	48.03
181-06	3.63	46.40	168.21	0.163	0.145	375.7	49.87
182-06	2.33	58.31	136.09	0.175	0.134	631.1	51.58
184-06	0.94	105.21	98.84	0.188	0.128	539.8	55.82
225-06	0.78	91.69	71.85	0.218	0.124	545.8	59.76
643-06	2.41	66.02	159.18	0.348	0.111	329.3	67.59

Table H-2. QLV parameters and percent relaxation of NT group.

	A	B	A*B	C	τ_1	τ_2	%
179-06	1.37	61.32	84.00	0.303	0.115	365.2	65.42
188-06	1.06	48.00	51.07	0.337	0.090	454.5	68.08
226-06	1.40	55.12	77.05	0.195	0.107	576.1	55.92
542-06	0.48	86.47	41.83	0.190	0.111	510.0	57.28
544-06	1.83	42.95	78.67	0.185	0.127	529.0	55.53
641-06	2.85	42.01	119.67	0.148	0.147	491.1	49.13

Table I-3. QLV parameters and percent relaxation of Sham group.

	A	B	A*B	C	τ_1	τ_2	%
179-06	10.43	58.58	610.86	0.096	0.144	521.2	37.06%
180-06	9.28	32.08	297.73	0.055	0.141	441.3	23.32%
181-06	9.26	36.27	335.91	0.060	0.143	518.6	26.56%
182-06	6.62	73.04	483.28	0.097	0.161	699.9	37.36%
184-60	2.01	50.94	102.29	0.265	0.090	350.7	60.60%
188-06	2.87	152.62	437.36	0.110	0.135	526.8	39.99%
225-06	7.76	55.01	426.89	0.112	0.123	471.9	38.95%
226-06	8.90	70.49	627.57	0.093	0.131	719.6	34.89%
542-06	3.57	48.53	173.23	0.073	0.145	614.8	31.45%
544-06	19.46	20.08	390.67	0.099	0.113	498.4	36.66%
641-06	7.31	64.67	472.48	0.065	0.173	670.5	28.98%
643-06	19.04	43.52	828.57	0.207	0.075	418.0	54.09%

BIBLIOGRAPHY

1. Abramowitch SD, Clineff TD, Debski RE, and Woo S.L-Y.. An experimental and analytical evaluation of the nonlinear viscoelastic properties of the healing medial collateral ligament in a goat model. In: *American Society of Mechanical Engineers, Bioengineering Division (Publication) BED*2003, p. 337-338.

2. Abramowitch SD, Papageorgiou CD, Debski RE, Clineff TD, and Woo S.L-Y.. A biomechanical and histological evaluation of the structure and function of the healing medial collateral ligament in a goat model. *Knee Surgery, Sports Traumatology, Arthroscopy* 11: 155-162, 2003.

3. Abramowitch SD, and Woo S.L-Y.. An improved method to analyze the stress relaxation of ligaments following a finite ramp time based on the quasi-linear viscoelastic theory. *Journal of Biomechanical Engineering* 126: 92-97, 2004.

4. Abramowitch SD, Woo S.L-Y., Clineff TD, and Debski RE. An evaluation of the quasi-linear viscoelastic properties of the healing medial collateral ligament in a goat model. *Annals of Biomedical Engineering* 32: 329-335, 2004.

5. Abramowitch SD, Yagi M, Tsuda E, and Woo S.L-Y.. The healing medial collateral ligament following a combined anterior cruciate and medial collateral ligament injury - A biomechanical study in a goat model. *Journal of Orthopaedic Research* 21: 1124-1130, 2003.

6. Abramowitch SD, Zhang J, Moon DK, and Woo S.L-Y.. The Effects of Porcine Small Intestine Submucosa
on the Viscoelastic Properties of Healing Medial Collateral Ligaments *Journal of Biomechanical Engineering title being written*: 2007.

7. Al Jamal R, Roughley PJ, and Ludwig MS. Effect of glycosaminoglycan degradation on lung tissue viscoelasticity. *American Journal of Physiology - Lung Cellular and Molecular Physiology* 280: L306-L315, 2001.

8. Allman AJ, McPherson TB, Badylak SF, Merrill LC, Kallakury B, Sheehan C, Raeder RH, and Metzger DW. Xenogeneic extracellular matrix grafts elicit a Th2-restricted immune response. *Transplantation* 71: 1631-1640, 2001.

9. Allman AJ, McPherson TB, Merrill LC, Badylak SF, and Metzger DW. The Th2-restricted immune response to xenogeneic small intestinal submucosa does not influence systemic protective immunity to viral and bacterial pathogens. *Tissue Engineering* 8: 53-62, 2002.

10. Badylak S, Liang A, Record R, Tullius R, and Jason H. Endothelial cell adherence to small intestinal submucosa: An acellular bioscaffold. *Biomaterials* 20: 2257-2263, 1999.

11. Badylak SF. Extracellular matrix as a scaffold for tissue engineering in veterinary medicine: Applications to soft tissue healing. *Clinical Techniques in Equine Practice* 3: 173-181, 2004.

12. Badylak SF. Xenogeneic extracellular matrix as a scaffold for tissue reconstruction. *Transplant Immunology* 12: 367-377, 2004.

13. Badylak SF, Arnoczky S, Plouhar P, Haut R, Mendenhall V, Clarke R, and Horvath C. Naturally occurring extracellular matrix as a scaffold for musculoskeletal repair. *Clinical Orthopaedics and Related Research* S333-S343, 1999.

14. Badylak SF, Tullius R, Kokini K, Shelbourne KD, Klootwyk T, Voytik SL, Kraine MR, and Simmons C. The use of xenogeneic small intestinal submucosa as a biomaterial for Achille's tendon repair in a dog model. *Journal of Biomedical Materials Research* 29: 977-985, 1995.

15. Birk DE, Fitch JM, Babiarz JP, Doane KJ, and Linsenmayer TF. Collagen fibrillogenesis in vitro: Interaction of types I and V collagen regulates fibril diameter. *Journal of Cell Science* 95: 649-657, 1990.

16. Birk DE, and Mayne R. Localization of collagen types I, III and V during tendon development. Changes in collagen types I and III are correlated with changes in fibril diameter. *European Journal of Cell Biology* 72: 352-361, 1997.

17. Bonifasi-Lista C, Lake SP, Small MS, and Weiss JA. Viscoelastic properties of the human medial collateral ligament under longitudinal, transverse and shear loading. *Journal of Orthopaedic Research* 23: 67-76, 2005.

18. Bray RC, Rangayyan RM, and Frank CB. Normal and healing ligament vascularity: A quantitative histological assessment in the adult rabbit medial collateral ligament. *Journal of Anatomy* 188: 87-95, 1996.

19. Carew EO, Talman EA, Boughner DR, and Vesely I. Quasi-linear viscoelastic theory applied to internal shearing of porcine aortic valve leaflets. *Journal of Biomechanical Engineering* 121: 386-392, 1999.

20. Chimich D, Frank C, Shrive N, Bray R, King G, and McDonald D. No effect of mop-ending on ligament healing. Rabbit studies of severed collateral knee ligaments. *Acta Orthopaedica Scandinavica* 64: 587-591, 1993.

21. Chimich D, Frank C, Shrive N, Dougall H, and Bray R. The effects of initial end contact on medial collateral ligament healing: A morphological and biomechanical study in a rabbit model. *Journal of Orthopaedic Research* 9: 37-47, 1991.

22. Chimich D, Shrive N, Frank C, Marchuk L, and Bray R. Water content alters viscoelastic behaviour of the normal adolescent rabbit medial collateral ligament. *Journal of Biomechanics* 25: 831-837, 1992.

23. Cobb MA, Badylak SF, Janas W, Simmons-Byrd A, and Boop FA. Porcine small intestinal submucosa as a dural substitute. *Surgical Neurology* 51: 99-104, 1999.

24. Cooper RR, and Misol S. Tendon and ligament insertion. A light and electron microscopic study. *Journal of Bone and Joint Surgery - Series A* 52: 1-20, 1970.

25. Dejardin LM, Arnoczky SP, Ewers BJ, Haut RC, and Clarke RB. Tissue-engineered rotator cuff tendon using porcine small intestine submucosa: Histologic and mechanical evaluation in dogs. *American Journal of Sports Medicine* 29: 175-184, 2001.

26. Doehring TC, Carew EO, and Vesely I. The effect of strain rate on the viscoelastic response of aortic valve tissue: A direct-fit approach. *Annals of Biomedical Engineering* 32: 223-232, 2004.

27. Dortmans LJMG, Sauren AAHJ, and Rousseau EPM. Parameter estimation using the quasi-linear viscoelastic model proposed by Fung. *Journal of Biomechanical Engineering* 106: 198-203, 1984.

28. Edson C. Postoperative rehabilitation of the multiple-ligament reconstructed knee. *Operative Techniques in Sports Medicine* 11: 294-301, 2003.

29. Edson CJ. Conservative and postoperative rehabilitation of isolated and combined injuries of the medial collateral ligament. *Sports Medicine and Arthroscopy Review* 14: 105-110, 2006.

30. Elliott DM, Robinson PS, Gimbel JA, Sarver JJ, Abboud JA, Iozzo RV, and Soslowsky LJ. Effect of altered matrix proteins on quasilinear viscoelastic properties in transgenic mouse tail tendons. *Annals of Biomedical Engineering* 31: 599-605, 2003.

31. Ellsasser J, Reynolds F, and Omohundro J. The nonoperative treatment of collateral ligament injuries of the knee in professional football players: An analysis of seventy-four injuries treated non-operatively and twenty-four injuries treated surgically. *Journal of Bone and Joint Surgery - Series A* 56: 1185-1190, 1974.

32. Fetto JF, and Marshall JL. Medial collateral ligament injuries of the knee: A rationale for treatment. *Clinical Orthopaedics and Related Research* NO.132: 206-218, 1978.

33. Figgie III HE, Bahniuk EH, Heiple KG, and Davy DT. The effects of tibial-femoral angle on the failure mechanics of the canine anterior cruciate ligament. *Journal of Biomechanics* 19: 89-91, 1986.

34. Fisher MB, Abramowitch S, and Woo S.L-Y.. New approach of QLV - effect of preload. In: *Summer Bioengineering Conference: American Society of Mechanical Engineers*. Amelia, FL: 2006.

35. Frank C, Woo S.L-Y., and Amiel D. Medial collateral ligament healing. A multidisciplinary assessment in rabbits. *American Journal of Sports Medicine* 11: 379-389, 1983.

36. Frank CB, Loitz B, Bray R, Chimich D, King G, and Shrive N. Abnormality of the contralateral ligament after injuries of the medial collateral ligament: An experimental study in rabbits. *Journal of Bone and Joint Surgery - Series A* 76: 403-412, 1994.

37. Frank CB, Loitz BJ, and Shrive NG. Injury location affects ligament healing: A morphologic and mechanical study of the healing rabbit medial collateral ligament. *Acta Orthopaedica Scandinavica* 66: 455-462, 1995.

38. Franklin Jr ME, Gonzalez Jr JJ, and Glass JL. Use of porcine small intestinal submucosa as a prosthetic device for laparoscopic repair of hernias in contaminated fields: 2-year follow-up. *Hernia* 8: 186-189, 2004.

39. Fukuta S, Oyama M, Kavalkovich K, Fu FH, and Niyibizi C. Identification of types II, IX and X collagens at the insertion site of the bovine Achilles tendon. *Matrix Biology* 17: 65-73, 1998.

40. Fung Y-C. *Biomechanics: Mechanical Properties of Living Tissues*. La Jolla, CA: Springer, 1993, p. 568.

41. Fung Y-C. Stress-Strain-History Relations of Soft Tissues in Simple Elongation. In: *Biomechanics: Its Foundations and Objectivs*. Englewood Cliffs, NJ: Prentice-Hall Inc., 1972, p. 181-208.

42. Funk JR, Hall GW, Crandall JR, and Pilkey WD. Linear and quasi-linear viscoelastic characterization of ankle ligaments. *Journal of Biomechanical Engineering* 122: 15-22, 2000.

43. Giannotti BF, Rudy T, and Graziano J. The non-surgical management of isolated medial collateral ligament injuries of the knee. *Sports Medicine and Arthroscopy Review* 14: 74-77, 2006.

44. Gomez MA, Woo S.L-Y., Inoue M, Amiel D, Harwood FL, and Kitabayashi L. Medial collateral ligament healing subsequent to different treatment regimens. *Journal of Applied Physiology* 66: 245-252, 1989.

45. Gomez MA, Woo S.L-Y., Amiel D, Harwood F, Kitabayashi L, and Matyas JR. Winner of the 1990 O'Donoghue award. The effects of increased tension on healing medial collateral ligaments. *American Journal of Sports Medicine* 19: 347-354, 1991.

46. Hart DP, and Dahners LE. Healing of the Medial Collateral Ligament in Rats. *Journal of Bone and Joint Surgery - Series A* 69-A: 1194-1199, 1987.

47. Hingorani RV, Provenzano PP, Lakes RS, Escarcega A, and Vanderby Jr R. Nonlinear viscoelasticity in rabbit medial collateral ligament. *Annals of Biomedical Engineering* 32: 306-312, 2004.

48. Hodde J. Review: Naturally occurring scaffolds for soft tissue repair and regeneration. *Tissue Engineering* 8: 295-308, 2002.

49. Hodde J, and Hiles M. Virus safety of a porcine-derived medical device: Evaluation of a viral inactivation method. *Biotechnology and Bioengineering* 79: 211-216, 2002.

50. Hodde J, Record R, Tullius R, and Badylak S. Fibronectin peptides mediate HMEC adhesion to porcine-derived extracellular matrix. *Biomaterials* 23: 1841-1848, 2002.

51. Hodde JP, and Hiles MC. Bioactive FGF-2 in Sterilized Extracellular Matrix. *Wounds* 13: 195-201, 2001.

52. Hodde JP, and Hiles MC. Immunological considerations of acellular xenogeneic scaffolds. In: *Third Smith and Nephew International Symposium - Translating Tissue Engineering into Products*2002, p. 41.

53. Hodde JP, Record RD, Liang HA, and Badylak SF. Vascular endothelial growth factor in porcine-derived extracellular matrix. *Endothelium: Journal of Endothelial Cell Research* 8: 11-24, 2001.

54. Indelicato P. Non-operative treatment of complete tears of the medial collateral ligament of the knee. *Journal of Bone and Joint Surgery - Series A* 65: 323-329, 1983.

55. Inoue M, McGurk-Burleson E, Hollis JM, and Woo S.L-Y.. Treatment of the medial collateral ligament injury. I: The importance of anterior cruciate ligament on the varus-valgus knee laxity. *American Journal of Sports Medicine* 15: 15-21, 1987.

56. Inoue M, Woo S.L-Y., Gomez MA, Amiel D, Ohland KJ, and Kitabayashi LR. Effects of surgical treatment and immobilization on the healing of the medial collateral ligament: a long-term multidisciplinary study. *Connective Tissue Research* 25: 13-26, 1990.

57. Jack E. Experimetnal rupture of the mdial collateral ligament of the knee. *Journal of Bone and Joint Surgery - Series B* 32: 396-402, 1950.

58. Kim SM, McCulloch TM, and Rim K. Comparison of viscoelastic properties of the pharyngeal tissue: Human and canine. *Dysphagia* 14: 8-16, 1999.

59. Kropp BP. Small-intestinal submucosa for bladder augmentation: A review of preclinical studies. *World Journal of Urology* 16: 262-267, 1998.

60. Kropp BP, Eppley BL, Prevel CD, Rippy MK, Harruff RC, Badylak SF, Adams MC, Rink RC, Keating MA, Gonzalez R, and Kropp BP. Experimental assessment of small intestinal submucosa as a bladder wall substitute. *Urology* 46: 396-400, 1995.

61. Kwan MK, Lin THC, and Woo S.L-Y.. On the viscoelastic properties of the anteromedial bundle of the anterior cruciate ligament. *Journal of Biomechanics* 26: 447-452, 1993.

62. Lantz GC, Badylak SF, Hiles MC, Coffey AC, Geddes LA, Kokini K, Sandusky GE, and Morff RJ. Small intestinal submucosa as a vascular graft: A review. *Journal of Investigative Surgery* 6: 297-310, 1993.

63. Laros GS, Tipton CM, and Cooper RR. Influence of physical activity on ligament insertions in the knees of dogs. *Journal of Bone and Joint Surgery - Series A* 53: 275-286, 1971.

64. Laws G, and Walton M. Fibroblastic healing of grade II ligament injuries: Histological and mechanical studies in the sheep. *Journal of Bone and Joint Surgery - Series B* 70: 390-396, 1988.

65. Lee T, and Woo S.L-Y.. A New Method for Determining Cross-Sectional Shape and Area of Soft Tissues. *Journal of Biomechanical Engineering* 110: 110-114, 1988.

66. Liang R, Nguyen T, Liu P, Carruthers C, Almarza A, and Woo S.L-Y.. A bioscaffold induces changes in the fibrillogenesis-related gene expressions in healing ligaments. *53rd Annual Meeting of the Orthopaedic Research Society* 2007.

67. Liang R, Woo S.L-Y., Takakura Y, Moon DK, Jia F, and Abramowitch SD. Long-term effects of porcine small intestine submucosa on the healing of medial collateral ligament: A functional tissue engineering study. *Journal of Orthopaedic Research* 24: 811-819, 2006.

68. Lindberg K, and Badylak SF. Porcine small intestinal submucosa (SIS): A bioscaffold supporting in vitro primary human epidermal cell differentiation and synthesis of basement membrane proteins. *Burns* 27: 254-266, 2001.

69. Linsenmayer TF, Gibney E, Igoe F, Gordon MK, Fitch JM, Fessler LI, and Birk DE. Type V collagen: Molecular structure and fibrillar organization of the chicken ?1(V) NH2-terminal domain, a putative regulator of corneal fibrillogenesis. *Journal of Cell Biology* 121: 1181-1189, 1993.

70. Loitz-Ramage BJ, Frank CB, and Shrive NG. Injury size affects long term strength of the rabbit medial collateral ligament. *Clinical Orthopaedics and Related Research* 272-280, 1997.

71. Majima T, Lo IKY, Marchuk LL, Shrive NG, and Frank CB. Effects of ligament repair on laxity and creep behavior of an early healing ligament scar. *Journal of Orthopaedic Science* 11: 272-277, 2006.

72. Mantovani F, Trinchieri A, Castelnuovo C, Romano AL, and Pisani E. Reconstructive Urethroplasty Using Porcine Acellular Matrix. *European Urology* 44: 600-602, 2003.

73. Matyas JR, Anton MG, Shrive NG, and Frank CB. Stress governs tissue phenotype at the femoral insertion of the rabbit MCL. *Journal of Biomechanics* 28: 147-157, 1995.

74. McPherson TB, Liang H, Record RD, and Badylak SF. Gal?(1,3)gal epitope in porcine small intestinal submucosa. *Tissue Engineering* 6: 233-239, 2000.

75. Miltner L, Hu C, and Fang H. Experimental joint sprain: Pathologic study. *Arch Surgery* 35: 1937.

76. Miyasaka K, Daniel D, Stone M, and Hirshman P. The Incidence of Knee Ligament Injuries in the General Population. *American Journal of Knee Surgery* 4: 3-8, 1991.

77. Moon DK, Abramowitch SD, and Woo S.L-Y.. The development and validation of a charge-coupled device laser reflectance system to measure the complex cross-sectional shape and area of soft tissues. *Journal of Biomechanics* 39: 3071-3075, 2006.

78. Moon DK, Woo S.L-Y., Takakura Y, Gabriel MT, and Abramowitch SD. The effects of refreezing on the viscoelastic and tensile properties of ligaments. *Journal of Biomechanics* 39: 1153-1157, 2006.

79. Musahl V, Abramowitch SD, Gilbert TW, Tsuda E, Wang JHC, Badylak SF, and Woo S.L-Y.. The use of porcine small intestinal submucosa to enhance the healing of the medial collateral ligament - A functional tissue engineering study in rabbits. *Journal of Orthopaedic Research* 22: 214-220, 2004.

80. Myers BS, McElhaney JH, Nighingale RW, and Doherty BJ. Quasi-linear modeling of the viscoelastic responses of the human cervical spine in torsion. In: *American Society of Mechanical Engineers, Bioengineering Division (Publication) BED*1991, p. 37-39.

81. Newton PO, Woo S.L-Y., Kitabayashi LR, Lyon RM, Anderson DR, and Akeson WH. Ultrastructrual changes in knee ligaments follwoing immobilization. *Matrix* 10: 314-319, 1990.

82. Nigul I, and Nigul U. On algorithms of evaluation of Fung's relaxation function parameters. *Journal of Biomechanics* 20: 343-352, 1987.

83. Niyibizi C, Kavalkovich K, Yamaji T, and Woo S.L-Y.. Type V collagen is increased during rabbit medial collateral ligament healing. *Knee Surgery, Sports Traumatology, Arthroscopy* 8: 281-285, 2000.

84. Niyibizi C, Sagarriga Visconti C, Gibson G, and Kavalkovich K. Identification and immunolocalization of type X collagen at the ligament-bone interface. *Biochemical and Biophysical Research Communications* 222: 584-589, 1996.

85. Niyibizi C, Visconti CS, Kavalkovich K, and Woo S.L-Y. Collagens in an adult bovine medial collateral ligament: Immunofluorescence localization by confocal microscopy reveals that type XIV collagen predominates at the ligament-bone junction. *Matrix Biology* 14: 743-751, 1995.

86. O'Connor RC, Hollowell CMP, and Steinberg GD. Distal ureteral replacement with tubularized porcine small intestine submucosa. *Urology* 60: 697x-697xii, 2002.

87. O'Donoghue D, Rockwood C, Zaricznyj B, and Kenyon R. Repair of knee ligaments in dogs: I-The lateral collateral ligament. *Journal of Bone and Joint Surgery - Series A* 43: 1167-1178, 1961.

88. Oakes B. Acute soft tissue injuris: nature and management. *Australian Family Physician* 10: 3-16, 1982.

89. Ohland KJ, Woo S.L-Y., Weiss JA, Takai S, and Shelley FJ. Healing of combined injuries of the rabbit medial collateral ligament and its insertions. A long term study on the effects of conservative vs. surgical treatment. In: *American Society of Mechanical Engineers, Bioengineering Division (Publication) BED*1991, p. 447-451.

90. Ohno K, Pomaybo AS, Schmidt CC, Levine RE, Ohland KJ, and Woo S.L-Y.. Healing of the medial collateral ligament after a combined medial collateral and anterior cruciate ligament injury and reconstruction of the anterior cruciate ligament: Comparison of repair and nonrepair of medial collateral ligament tears in rabbits. *Journal of Orthopaedic Research* 13: 442-449, 1995.

91. Piper TL, and Whiteside LA. Early Mobilization after Knee Ligament Repair in Dogs: An Experimental Study. *Clinical Orthopaedics and Related Research* 150: 277-282, 1980.

92. Prevel CD, Eppley BL, Summerlin DJ, Jackson JR, McCarty M, and Badylak SF. Small intestinal submucosa: Utilization for repair of rodent abdominal wall defects. *Annals of Plastic Surgery* 35: 374-380, 1995.

93. Provenzano P, Lakes R, Keenan T, and Vanderby R, Jr. Nonlinear ligament viscoelasticity. *Annals of Biomedical Engineering* 29: 908-914, 2001.

94. Provenzano PP, Lakes RS, Corr DT, and R Jr R. Application of nonlinear viscoelastic models to describe ligament behavior. *Biomechanics and modeling in mechanobiology* 1: 45-57, 2002.

95. Rodeo SA, and Izawa K. Tendon-to-bone healing: Basic science aspects and enhancement techniques. *Techniques in Orthopaedics* 14: 22-33, 1999.

96. Scheffler SU, Clineff TD, Papageorgiou CD, Debski RE, Ma CB, and Woo S.L-Y. Structure and function of the healing medial collateral ligament in a goat model. *Annals of Biomedical Engineering* 29: 173-180, 2001.

97. Schmidt MB, Mow VC, Chun LE, and Eyre DR. Effects of proteoglycan extraction on the tensile behavior of articular cartilage. *Journal of Orthopaedic Research* 8: 353-363, 1990.

98. Shirakura K, Terauchi M, Katayama M, Watanabe H, Yamaji T, and Takagishi K. The management of medial ligament team in patients with combined anterior cruciate and medial ligament lesions. *International Orthopaedics* 24: 108-111, 2000.

99. Shrive N, Chimich D, Marchuk L, Wilson J, Brant R, and Frank C. Soft-tissue 'flaws' are associated with the material properties of the healing rabbit medial collateral ligament. *Journal of Orthopaedic Research* 13: 923-929, 1995.

100. Simon BR, Coats RS, and Woo S.L-Y. Relaxation and creep quasilinear viscoelastic models for normal articular cartilage. *Journal of Biomechanical Engineering* 106: 159-164, 1984.

101. Song BZ, Donoff RB, Tsuji T, Todd R, Gallagher GT, and Wong DTW. Identification of rabbit eosinophils and heterophils in cutaneous healing wounds. *Histochemical Journal* 25: 762-771, 1993.

102. Strange PS. Small intestinal submucosa for laparoscopic repair of large paraesophageal hiatal hernias: a preliminary report. *Surgical technology international* 11: 141-143, 2003.

103. Tanaka R, Al-Jamal R, and Ludwig MS. Maturational changes in extracellular matrix and lung tissue mechanics. *Journal of Applied Physiology* 91: 2314-2321, 2001.

104. Thomopoulos S, Williams GR, and Soslowsky LJ. Tendon to bone healing: Differences in biomechanical, structural, and compositional properties due to a range of activity levels. *Journal of Biomechanical Engineering* 125: 106-113, 2003.

105. Voytik-Harbin SL, Brightman AO, Kraine MR, Waisner B, and Badylak SF. Identification of extractable growth factors from small intestinal submucosa. *Journal of Cellular Biochemistry* 67: 478-491, 1997.

106. Walsh S, and Frank C. Two methods of ligament injury: A morphological comparison in a rabbit model. *Journal of Surgical Research* 45: 159-166, 1988.

107. Wang JHC, and Grood ES. The strain magnitude and contact guidance determine orientation response of fibroblasts to cyclic substrate strains. *Connective Tissue Research* 41: 29-36, 2000.

108. Weiss JA, Woo S.L-Y., Ohland KJ, Horibe S, and Newton PO. Evaluation of a new injury model to study medial collateral ligament healing: Primary repair versus nonoperative treatment. *Journal of Orthopaedic Research* 9: 516-528, 1991.

109. Woo S.L-Y., Abramowitch SD, Kilger R, and Liang R. Biomechanics of knee ligaments: Injury, healing, and repair. *Journal of Biomechanics* 39: 1-20, 2006.

110. Woo S.L-Y., Danto M, Ohland KJ, Lee T, and Newton PO. The Use of a Laser Micrometer System to Determine the Cross-Sectional Shape and Area of Ligaments: A Comparative Study with Wto Existion Methods. *Journal of Biomechanical Engineering* 112: 426-431, 1990.

111. Woo S.L-Y., Gomez M, Seguchi Y, Endo C, and Akeson W. Measurement of Mechanical Properties of Ligament Substance from a Bone-Ligament-Bone Preparation. . *Journal of Orthopaedic Research* 1: 22-29, 1983.

112. Woo S.L-Y., and Buckwalter JA. AAOS/NIH/ORS workshop. Injury and repair of the musculoskeletal soft tissues. Savannah, Georgia, June 18-20, 1987. *Journal of orthopaedic research : official publication of the Orthopaedic Research Society* 6: 907-931, 1988.

113. Woo S.L-Y. Mechanical properties of tendons and ligaments. I. Quasi-static and nonlinear viscoelastic properties. *Biorheology* 19: 385-396, 1982.

114. Woo S.L-Y., Gomez MA, and Akeson WH. The time and history-dependent viscoelastic properties of the canine medial collateral ligament. *Journal of Biomechanical Engineering* 103: 293-298, 1981.

115. Woo S.L-Y., Gomez MA, and Amiel D. The effects of exercise on the biomechanical and biochemical properties of swine digital flexor tendons. *Journal of Biomechanical Engineering* 103: 51-56, 1981.

116. Woo S.L-Y., Gomez MA, Sites TJ, Newton PO, Orlando CA, and Akeson WH. The biomechanical and morphological changes in the medial collateral ligament of the rabbit after immobilization and remobilization. *Journal of Bone and Joint Surgery - Series A* 69: 1200-1211, 1987.

117. Woo S.L-Y., Gomez MA, Woo YK, and Akeson WH. Mechanical properties of tendons and ligaments. II. The relationships of immobilization and exercise on tissue remodeling. *Biorheology* 19: 397-408, 1982.

118. Woo S.L-Y., Inoue M, McGurk-Burleson E, and Gomez MA. Treatment of the medial collateral ligament injury. II: Structure and function of canine knees in response to differing treatment regimens. *American Journal of Sports Medicine* 15: 22-29, 1987.

119. Woo S.L-Y., Peterson RH, Ohland KJ, Sites TJ, and Danto MI. The effects of strain rate on the properties of the medial collateral ligament in skeletally immature and mature rabbits: A biomechanical and histological study. *Journal of Orthopaedic Research* 8: 712-721, 1990.

120. Woo S.L-Y., Young EP, Ohland KJ, Marcin JP, Horibe S, and Lin HC. The effects of transection of the anterior cruciate ligament on healing of the medical collateral ligament. A

biomechanical study of the knee in dogs. *Journal of Bone and Joint Surgery - Series A* 72: 382-392, 1990.

121. Yamaji T, Levine RE, Woo SLY, Niyibizi C, Kavalkovich KW, and Weaver- Green CM. Medial collateral ligament healing one year after a concurrent medial collateral ligament and anterior cruciate ligament injury: An interdisciplinary study in rabbits. *Journal of Orthopaedic Research* 14: 223-227, 1996.

122. Zaffagnini S, Bignozzi S, Martelli S, Lopomo N, and Marcacci M. Does ACL reconstruction restore knee stability in combined lesions? An in vivo study. *Clinical Orthopaedics and Related Research* 95-99, 2007.

123. Zheng YP, and Mak AFT. Extraction of quasi-linear viscoelastic parameters for lower limb soft tissues from manual indentation experiment. *Journal of Biomechanical Engineering* 121: 330-339, 1999.